

Adaptive Robot Navigation with Collision Avoidance Subject to 2nd-order Uncertain Dynamics

Christos K. Verginis and Dimos V. Dimarogonas

KTH Royal Institute of Technology, School of Electrical
Engineering and Computer Science
{cverginis,dimos}@kth.se

Abstract

This paper considers the problem of robot motion planning in a workspace with obstacles for systems with uncertain 2nd-order dynamics. In particular, we combine closed form potential-based feedback controllers with adaptive control techniques to guarantee the collision-free robot navigation to a predefined goal while compensating for the dynamic model uncertainties. We base our findings on sphere world-based configuration spaces, but extend our results to arbitrary star-shaped environments by using previous results on configuration space transformations. Moreover, we propose an algorithm for extending the control scheme to decentralized multi-robot systems. Finally, extensive simulation results verify the theoretical findings.

1 Introduction

Motion planning and specifically robotic navigation in obstacle-cluttered environments is a fundamental problem in the field of robotics [1]. Several techniques have been developed in the related literature, such as discretization of the continuous space and employment of discrete algorithms (e.g., Dijkstra, A^*), probabilistic roadmaps, sampling-based motion planning, and

feedback-based motion planning [2]. The latter, which is the focus of the current paper, offers closed-form analytic solutions by usually evaluating appropriately designed artificial potential fields, avoiding thus the potential complexity of workspace discretization and the respective algorithms. At the same time, feedback-based methods provide a solution to the control aspect of the motion planning problem, i.e., the correctness based on the solution of the closed-loop differential equation that describes the robot model.

Early works on feedback-based motion planning established the Koditschek-Rimon navigation function (KRNF) [3, 4], where, through gain tuning, the robot converges safely to its goal from almost all initial conditions (in the sense of a measure-zero set). KRNFs were extended to more general workspaces and adaptive gain controllers [5], to multi-robot systems [6–9], and more recently, to convex potential and obstacles [10]. The idea of gain tuning has been also employed to an alternative KRNF in [11]. Tuning-free constructions of artificial potential fields have also been developed in the related literature; [12] tackles nonholonomic multi-robot systems, and in [13, 14] harmonic functions, also used in [15], are combined with adaptive controllers to achieve almost global safe navigation. A transformation of arbitrarily shaped worlds to points worlds, which facilitates the motion planning problem, is also considered in [13, 14] and in [16] for multi-robot systems. The recent works [13], [17] guarantee also safe navigation in predefined *time*.

Barrier functions for multi-robot collision avoidance are employed in [18] and optimization-based techniques via model predictive control (MPC) can be found in [19–22]; [23] and [24] propose reciprocal collision obstacle by local decision making for the desired velocity of the robot(s). Ellipsoidal obstacles are tackled in [25] and [26] extends a given potential field to 2nd-order systems. A similar idea is used in [27], where the effects of an unknown drift term in the dynamics are examined. Workspace decomposition methodologies with hybrid controllers are employed in [28], [29], and [30], and [31] employs a contraction-based methodology that can also tackle the case of moving obstacles.

A common assumption that most of the aforementioned works consider is the simplified robot dynamics, i.e., single integrators/unicycle kinematics, without taking into account any robot dynamic parameters. Hence, indirectly, the schemes depend on an embedded internal system that converts the desired velocity signal to the actual robot actuation command. The above imply that the actual robot trajectory might deviate from the desired one, jeopardizing its safety and possibly resulting in collisions. Second-order

realistic robot models are considered in MPC-schemes, like [19–21], which might, however, result in computationally expensive solutions. Moreover, regarding model uncertainties, a global upper bound is required, which is used to enlarge the obstacle boundaries and might yield infeasible solutions. A 2nd-order model is considered in [25], [26], without, however, considering any unknown dynamic terms. The works [6, 32–34] consider simplified 2nd-order systems with *known* dynamic terms (and in particular, inertia and gravitational terms that are assumed to be successfully compensated); [27] guarantees the asymptotic stability of 2nd-order systems with a class of unknown drift terms to the critical points of a given potential function. However, there is no characterization of the region of attraction of the goal. Adaptive control for constant unknown parameters is employed in [35], where a swarm of robots is controlled to move inside a desired region.

In this paper, we consider the robot navigation in an obstacle-cluttered environment under 2nd-order uncertain robot dynamics, in terms of unknown mass and friction/drag terms. Our main contribution lies in the design of a novel 2nd-order smooth navigation function as well as an adaptive control law that guarantees the *safe* navigation of the robot from almost all initial conditions. We also show how the proposed scheme can be applied to star-worlds, i.e., workspaces with star-shaped obstacles [4], as well as to decentralized multi-robot navigation. Adaptive control for multi-robot coordination was also employed in our previous works [8, 36]. The results in [8], however, are only existential, since we do not provide an explicit potential function that satisfies the desired properties, while [36] focuses on the multi-agent ellipsoidal collision avoidance, without guaranteeing achievement of the primary task.

The rest of the paper is organized as follows. Section 2 provides the notation used throughout the paper. Section 3 describes the tackled problem and Section 4 provides the main results. Sections 5 and 6 extend the proposed scheme to star worlds and multi-agent frameworks, respectively. Finally, simulation studies are given in Section 7 and Section 8 concludes the paper.

2 Notation

The set of natural and real numbers is denoted by \mathbb{N} , and \mathbb{R} , respectively, and $\mathbb{R}_{\geq 0}^n$, $\mathbb{R}_{>0}^n$, $n \in \mathbb{N}$, are the n -dimensional sets of nonnegative and positive real numbers, respectively. The notation $\|x\|$ implies the Euclidean norm of a

vector $x \in \mathbb{R}^n$. The identity matrix is denoted by $I_n \in \mathbb{R}^{n \times n}$, the $n \times m$ matrix of zeros by $0_{n \times m}$ and the n -dimensional zero vector by 0_n . The gradient and Hessian of a function $f : \mathbb{R}^n \rightarrow \mathbb{R}$ are denoted by $\nabla_x f(x) := \frac{\partial f(x)}{\partial x} \in \mathbb{R}^n$ and $\nabla_x^2 f(x) \in \mathbb{R}^{n \times n}$, respectively.

3 Problem Statement

Consider a spherical robot operating in a bounded workspace \mathcal{W} , characterized by its position vector $x \in \mathbb{R}^n$, $n \in \{2, 3\}$ and radius $r > 0$, and subject to the dynamics:

$$\dot{x} = v \tag{1a}$$

$$m\dot{v} + f(x, v) + mg = u, \tag{1b}$$

where $m > 0$ is the *unknown* mass, $g \in \mathbb{R}^n$ is the constant gravity vector, $u \in \mathbb{R}^n$ is the input vector, and $f : \mathbb{R}^{2n} \rightarrow \mathbb{R}^n$ is an *unknown* friction-like function, satisfying the following assumption:

Assumption 1 *The function $f : \mathbb{R}^{2n} \rightarrow \mathbb{R}^n$ is analytic and satisfies*

$$\|f(x, v)\| \leq \alpha \|v\|, \tag{2}$$

$\forall x, v \in \mathbb{R}^{2n}$, where $\alpha \in \mathbb{R}_{\geq 0}$ is an unknown constant.

The aforementioned assumption is inspired by standard friction-like terms, which can be approximated by continuously differentiable velocity functions [37]. Constant unknown friction terms could be also included in the dynamics (e.g., incorporated in the constant gravity vector). Note also that $\|f(x, v)\| \leq \alpha \|v\|$ implies $f(x, 0_n) = 0_n$, and $\frac{\partial f(x, v)}{\partial x} \Big|_{v=0_n} = 0_{n \times n}$. The workspace is assumed to be an open ball centered at the origin

$$\mathcal{W} := \{q \in \mathbb{R}^n : \|q\| < r_{\mathcal{W}}\}, \tag{3}$$

where $r_{\mathcal{W}} > 0$ is the workspace radius. The workspace contains $M \in \mathbb{N}$ closed sets \mathcal{O}_j , $j \in \mathcal{J} := \{1, \dots, M\}$, corresponding to obstacles. Each obstacle is a closed ball centered at $c_j \in \mathbb{R}^3$, with radius $r_{o_j} > 0$, i.e., $\mathcal{O}_j := \{q \in \mathcal{W} :$

$\|q - c_j\| \leq r_{o_j}\}$, $\forall j \in \mathcal{J}$. The analysis that follows will be based on the transformed workspace:

$$\bar{\mathcal{W}} := \{q \in \mathbb{R}^n : \|q\| < \bar{r}_{\mathcal{W}} := r_{\mathcal{W}} - r\}, \quad (4)$$

and set of obstacles $\bar{\mathcal{O}}_j := \{q \in \mathcal{W} : \|q - c_j\| \leq \bar{r}_{o_j} := r_{o_j} + r\}$, $\forall j \in \mathcal{J}$, where the robot is reduced to the point x . The free space is defined as

$$\mathcal{F} := \bar{\mathcal{W}} \setminus \bigcup_{j \in \mathcal{J}} \bar{\mathcal{O}}_j, \quad (5)$$

also known as a *sphere world* [3]. We consider the following common feasibility assumption [3, 17] for \mathcal{F} :

Assumption 2 *The workspace \mathcal{W} and the obstacles \mathcal{O}_j satisfy $\|c_i - c_j\| > r_{o_i} + r_{o_j} + 2r$ and $r_{\mathcal{W}} - \|c_j\| > r_{o_j} + 2r$, $\forall i, j \in \mathcal{J}, i \neq j$.*

Assumption 2 implies that we can find some $\bar{r} > 0$ such that

$$\|c_i - c_j\| > r_{o_i} + r_{o_j} + 2r + 2\bar{r}, \quad \forall i, j \in \mathcal{J}, i \neq j, \quad (6a)$$

$$r_{\mathcal{W}} - \|c_j\| > r_{o_j} + 2r + 2\bar{r}, \quad \forall j \in \mathcal{J} \quad (6b)$$

This paper treats the problem of navigating the robot to a destination x_d while avoiding the obstacles and the workspace boundary, formally stated as follows:

Problem 1 *Consider a robot subject to the uncertain dynamics (1), operating in the aforementioned sphere world, with $(x(t_0), v(t_0)) \in \mathcal{F} \times \mathbb{R}^n$. Given a destination $x_d \in \mathcal{F}$, design a control protocol u such that*

$$\begin{aligned} x(t) &\in \mathcal{F}, \quad t \geq t_0 \\ \lim_{t \rightarrow \infty} (x(t), v(t)) &= (x_d, 0_n) \end{aligned}$$

4 Main Results

We provide in this section our methodology for solving Problem 1. Define first the set $\bar{\mathcal{J}} := \{0\} \cup \mathcal{J}$ as well as the distances $d_j : \mathcal{F} \rightarrow \mathbb{R}_{\geq 0}$, $j \in \bar{\mathcal{J}}$, with $d_j(x) := \|x - c_j\|^2 - \bar{r}_{o_j}^2$, $\forall j \in \mathcal{J}$, and $d_0(x) := \bar{r}_{\mathcal{W}}^2 - \|x\|^2$. Note that,

by keeping $d_j(x) > 0$, $d_0(x) > 0$, we guarantee that $x \in \mathcal{F}^1$. We also define the constant

$$\bar{r}_d := \min \left\{ \bar{r}_{\mathcal{W}}^2 - \|x_d\|^2, \min_{j \in \bar{\mathcal{J}}} \{d_j(x_d)\} \right\} \quad (7)$$

as the minimum distance of the goal to the obstacles/workspace boundary. We introduce next the notion of the *2nd-order navigation function*:

Definition 1 *A 2nd-order navigation function is a function $\phi : \mathcal{F} \rightarrow \mathbb{R}_{\geq 0}$ of the form*

$$\phi(x) := k_1 \|x - x_d\|^2 + k_2 \sum_{j \in \bar{\mathcal{J}}} \beta(d_j(x)),$$

where $\beta : \mathbb{R}_{>0} \rightarrow \mathbb{R}_{\geq 0}$ is a (at least) twice contin. differentiable function and k_1, k_2 are positive constants, with the followings properties:

1. $\beta((0, \tau])$ is strictly decreasing, $\lim_{z \rightarrow 0} \beta(z) = \infty$, and $\beta(z) = \beta(\tau)$, $\forall z \geq \tau$, $j \in \bar{\mathcal{J}}$, for some $\tau > 0$,
2. $\phi(x)$ has a global minimum at $x = x_d \in \text{int}(\mathcal{F})$ where $\phi(x_d) = 0$,
3. if $\beta'(d_k(x)) \neq 0$ and $\beta''(d_k(x)) \neq 0$ for some $k \in \bar{\mathcal{J}}$, then $\beta'(d_j(x)) = \beta''(d_j(x)) = 0$, for all $j \in \bar{\mathcal{J}} \setminus \{k\}$.
4. The function $\tilde{\beta} : (0, \tau) \rightarrow \mathbb{R}_{\geq 0}$, with $\tilde{\beta}(z) := \beta''(z)z\sqrt{z}$ is strictly decreasing.

By using the first property we will guarantee that, by keeping $\beta(d_j(x))$ bounded, there are no collisions with the obstacles or the free space boundary. Property 2 will be used for the asymptotic stability of the desired point $x = x_d$. Property 3 places the rest of the critical points of ϕ (which are proven to be saddle points) close to the obstacles, and the last property is used to guarantee that these are non-degenerate. An example for β that satisfies properties 1) and 4), is

$$\beta(z) := \begin{cases} (6z^5 - 15z^4 + 10z^3)^{-1}, & z \leq 1 \\ 1, & z \geq 1, \end{cases} \quad (8)$$

¹A safety margin can also be included, which needs, however, to be incorporated in the constant \bar{r} of (6).

Note that β is essentially a reciprocal barrier function [18]. We prove next that, by appropriately choosing τ , only one $\beta(d_j(x))$, $j \in \bar{\mathcal{J}}$ affects the robotic agent for each $x \in \mathcal{F}$, and furthermore that $\beta'(d_j(x_d)) = \beta''(d_j(x_d)) = 0$. Hence, properties 2) and 3) of Def. 1 are satisfied.

Proposition 1 *By choosing τ as $\tau \in (0, \min\{\bar{r}^2, \bar{r}_d\})$, where \bar{r}, \bar{r}_d were introduced in (6) and (7), respectively, we guarantee that at each $x \in \mathcal{F}$ there is no more than one $j \in \bar{\mathcal{J}}$ such that $d_j \leq \tau$, implying that $\beta'(d_j(x))$ and $\beta''(d_j(x))$ are non-zero.*

Proof Assume that $d_j(x) \leq \tau$ for some $j \in \mathcal{J}$, $x \in \mathcal{F}$. Then, in view of (6), it holds that

$$\|x - c_j\|^2 < \bar{r}^2 + \bar{r}_{o_j}^2 \Rightarrow \|x - c_j\| < \bar{r} + \bar{r}_{o_j} = \bar{r} + r + r_{o_j} < \|c_j - c_k\|$$

$\forall k \in \mathcal{J} \setminus \{j\}$, and hence

$$\begin{aligned} \|x - c_k\| &= \|x - c_j + c_j - c_k\| \geq \|c_j - c_k\| - \|x - c_j\| > r_{o_k} + r + \bar{r} \Rightarrow \\ \|x - c_k\|^2 &> (r_{o_k} + r + \bar{r})^2 > (r_{o_k} + r)^2 + \bar{r}^2, \end{aligned}$$

implying $d_k(x) > \bar{r}^2 > \tau$, $\forall k \in \mathcal{J} \setminus \{j\}$. Moreover, in view of (6), it holds that

$$\begin{aligned} \|x\| &\leq \|x - c_j\| + \|c_j\| \pm r_{\mathcal{W}} \Rightarrow \\ \|x\| &< r_{\mathcal{W}} - r - \bar{r} \Rightarrow (r_{\mathcal{W}} - r)^2 \geq (\|x\| + \bar{r})^2 \Rightarrow \\ \bar{r}_{\mathcal{W}}^2 &\geq \|x\|^2 + \bar{r}^2 \Rightarrow \bar{r}_{\mathcal{W}}^2 - \|x\|^2 > \bar{r}^2, \end{aligned}$$

and hence $d_o(x) > \tau$. Similarly, we conclude by contradiction that $d_o(x) \leq \tau \Rightarrow d_j > \tau$, $\forall j \in \mathcal{J}$.

Moreover, it holds for the desired equilibrium that

$$x = x_d \Leftrightarrow d_j(x) = \|x_d - c_j\|^2 - \bar{r}_j^2 \geq \bar{r}_d > \tau,$$

and

$$x = x_d \Leftrightarrow d_0(x) = \bar{r}_{\mathcal{W}}^2 - \|x_d\|^2 \geq \bar{r}_d > \tau,$$

and hence $\beta'(d_j(x_d)) = \beta''(d_j(x_d)) = 0$, $\forall j \in \bar{\mathcal{J}}$.

Intuitively, the obstacles and the workspace boundary have a local region of influence defined by the constant τ , which will play a significant role in

determining the stability of the overall scheme later. This robot interaction with only one obstacle at a time has also been demonstrated in the feedback control-based related literature, e.g., [5, 10, 17, 28, 38], which deals with simplified single-integrator models, as well as in the more discrete decision making *bug* algorithms [1], which involve circumnavigation of obstacles and can handle in general complex unknown environments.

The expressions for the gradient and the Hessian of ϕ , which will be needed later, are the following:

$$\nabla_x \phi(x) = 2k_1(x - x_d) + 2k_2 \sum_{j \in \mathcal{J}} \beta'(d_j)(x - c_j) - 2k_2 \beta'(d_0)x \quad (9a)$$

$$\begin{aligned} \nabla_x^2 \phi(x) = & 2 \left(k_1 - k_2 \beta'(d_0) + k_2 \sum_{j \in \mathcal{J}} \beta'(d_j) \right) I_n - 2k_2 \beta''(d_0) x x^\top + \\ & 2k_2 \sum_{j \in \mathcal{J}} \beta''(d_j)(x - c_j)(x - c_j)^\top. \end{aligned} \quad (9b)$$

Given the aforementioned definitions, we design a reference signal $v_d : \mathcal{F} \rightarrow \mathbb{R}^n$ for the robot velocity v as

$$v_d(x) = -\nabla_x \phi(x). \quad (10)$$

Next, we design the control input u to guarantee tracking of the aforementioned reference velocity as well as compensation of the unknown terms m and $f(x, v)$. More specifically, we define the signals $\hat{m} \in \mathbb{R}$ and $\hat{\alpha} \in \mathbb{R}$ as the estimation terms of m and α (see Assumption 1), respectively, and the respective errors $\tilde{m} := \hat{m} - m$, $\tilde{\alpha} := \hat{\alpha} - \alpha$. We design now the control law $u : \mathcal{F} \times \mathbb{R}^{n+2} \rightarrow \mathbb{R}^n$ as $u := u(x, v, \hat{m}, \hat{\alpha})$, with

$$u := -k_\phi \nabla_x \phi(x) + \hat{m}(\dot{v}_d + g) - \left(k_v + \frac{3}{2} \hat{\alpha} \right) e_v, \quad (11)$$

where $e_v := v - v_d$, and k_v , k_ϕ are positive gain constants. Moreover, we design the adaptation laws for the estimation signals as

$$\dot{\hat{m}} := -k_m e_v^\top (\dot{v}_d + g) \quad (12a)$$

$$\dot{\hat{\alpha}} := k_\alpha \|e_v\|^2, \quad (12b)$$

with k_m, k_α positive gain constants, $\hat{\alpha}(t_0) \geq 0$, and arbitrary finite initial condition $\hat{m}(t_0)$. As will be verified by the proof of Theorem 1, the choices for the control and adaptation laws are based on Lyapunov techniques, and follow standard adaptive control methodologies (see, e.g., [39]).

Theorem 1 *Consider a robot operating in \mathcal{W} , subject to the uncertain 2nd-order dynamics (1). Given $x_d \in \mathcal{F}$, the control protocol (10)-(12) guarantees the collision-free navigation to x_d from almost all initial conditions $(x(t_0), v(t_0), \hat{m}(t_0), \hat{\alpha}(t_0)) \in \mathcal{F} \times \mathbb{R}^{n+1} \times \mathbb{R}_{\geq 0}$, given a sufficiently small τ and that $k_\phi > \frac{\alpha}{2}$. Moreover, all closed loop signals remain bounded, $\forall t \geq t_0$.*

Proof *Consider the Lyapunov candidate function*

$$V := k_\phi \phi + \frac{m}{2} \|e_v\|^2 + \frac{3}{4k_\alpha} \tilde{\alpha}^2 + \frac{1}{2k_m} \tilde{m}^2. \quad (13)$$

Since $x(t_0) \in \mathcal{F}$, there exists a constant \bar{d}_j such that $d_j(x(t_0)) \geq \bar{d}_j > 0$, $j \in \bar{\mathcal{J}}$, and hence there exists a finite positive constant \bar{V}_0 such that $V(t_0) \leq \bar{V}_0$. By considering the time derivative of V and using $v = e_v + v_d$ and Assumption 1, we obtain after substituting (12):

$$\begin{aligned} \dot{V} &= k_\phi \nabla_x \phi(x)^\top (e_v + v_d) + e_v^\top (u - mg - f(x, v) - m\dot{v}_d) \\ &\quad + \frac{3}{2} \tilde{\alpha} \|e_v\|^2 - \tilde{m} e_v^\top (\dot{v}_d + g) \\ &\leq -k_\phi \|\nabla_x \phi(x)\|^2 + e_v^\top (k_\phi \nabla_x \phi(x) + u - m(g + \dot{v}_d)) + \\ &\quad \alpha \|e_v\| \|v\| + \frac{3}{2} \tilde{\alpha} \|e_v\|^2 - \tilde{m} e_v^\top (\dot{v}_d + g), \end{aligned}$$

which, by substituting (11) and using $\alpha \|e_v\| \|v\| \leq \frac{\alpha}{2} \|e_v\|^2 + \frac{\alpha}{2} \|\nabla_x \phi(x)\|^2 + \frac{\alpha}{2} \|e_v\|^2$, becomes

$$\begin{aligned} \dot{V} &\leq -\left(k_\phi - \frac{\alpha}{2}\right) \|\nabla_x \phi(x)\|^2 - \frac{3}{2} \hat{\alpha} \|e_v\|^2 + \frac{3}{2} \alpha \|e_v\|^2 \\ &\quad - k_v \|e_v\|^2 + \tilde{m} e_v^\top (g + \dot{v}_d) + \tilde{\alpha} \|e_v\|^2 - \tilde{m} e_v^\top (\dot{v}_d + g) \\ &= -\left(k_\phi - \frac{\alpha}{2}\right) \|\nabla_x \phi(x)\|^2 - k_v \|e_v\|^2 \leq 0. \end{aligned}$$

Hence, we conclude that $V(t)$ is non-increasing, and hence $\beta(d_j(x(t))) \leq V(t) \leq V(t_0) \leq \bar{V}_0$, $\forall t \geq t_0$, which implies that collisions with the obstacles and the workspace boundary are avoided, i.e.,

$$x(t) \in \bar{\mathcal{F}} := \{x \in \mathcal{F} : \beta(d_j(x)) \leq \bar{V}_0, \forall j \in \bar{\mathcal{J}}\},$$

$\forall t \geq t_0$. Moreover, (9) implies also the boundedness of $\nabla_x \phi(x)|_{x(t)}$, $\forall t \geq t_0$. In addition, the boundedness of $V(t)$ implies also the boundedness of $x(t)$, $e_v(t)$, $\tilde{m}(t)$, $\tilde{\alpha}(t)$, $\tilde{g}(t)$ and hence of $v(t)$, $\hat{m}(t)$, $\hat{\alpha}(t)$, $\forall t \geq t_0$. More specifically, by letting $s := [x^\top, v^\top, \tilde{\alpha}, \tilde{m}]^\top$, we conclude that $s(t) \in \bar{S}$, $\forall t \geq t_0$, with

$$\begin{aligned} \bar{S} := & \{s \in \bar{\mathcal{F}} \times \mathbb{R}^{n+2} : |\tilde{\alpha}| \leq \sqrt{\frac{4}{3}k_\alpha \bar{V}_0}, |\tilde{m}| \leq \sqrt{2k_m \bar{V}_0}, \\ & \|v\| \leq \sqrt{2m \bar{V}_0} + \sup_{x \in \bar{\mathcal{F}}} \|\nabla_x \phi(x)\|\} \end{aligned}$$

Therefore, by invoking LaSalle's invariance principle, we conclude that the solution $s(t)$ will converge to the largest invariant set in $S := \{s \in \bar{S} : \dot{V} = 0\}$, which, in view of (10), becomes $S := \{s \in \bar{S} : \nabla_x \phi(x) = 0, v = 0\}$. Consider now the closed-loop dynamics for s :

$$\dot{x} = v \tag{14a}$$

$$\dot{v} = \frac{1}{m}(\tilde{m}g + \hat{m}\dot{v}_d - k_\phi \nabla_x \phi(x) - f(x, v) - \left(k_v + \frac{3}{2}\hat{\alpha}\right)(v + \nabla_x \phi(x))) \tag{14b}$$

$$\dot{\tilde{m}} = -k_m(v + \nabla_x \phi(x))^\top (\dot{v}_d + g) \tag{14c}$$

$$\dot{\tilde{\alpha}} = k_\alpha \|v + \nabla_x \phi(x)\|^2. \tag{14d}$$

Note that, in view of the aforementioned discussion and the continuous differentiability of $f(x, v)$, the right-hand side of (14b) is bounded in \bar{S} . Note also that (9) implies the boundedness of $\nabla_x^2 \phi(x)$ in $\bar{\mathcal{F}}$. Moreover, by differentiating \dot{v} , using the closed loop dynamics (14) and (9), we conclude the boundedness of \ddot{v} and the uniform continuity of $\dot{v}(t)$ in \bar{S} . Hence, since $\lim_{t \rightarrow \infty} v(t) = 0$, we invoke Barbalat's Lemma to conclude $\lim_{t \rightarrow \infty} \dot{v}(t) = 0$.

Therefore, the set S consists of the points where $\dot{v} = v = \nabla_x \phi(x) = 0$, $\dot{v}_d = \nabla_x^2 \phi(x)v = 0$, and by also using the property $f(x, 0) = 0$ we obtain $\lim_{t \rightarrow \infty} \tilde{m}(t) = 0$ and $\lim_{t \rightarrow \infty} \dot{s}(t) = 0$. Note also that $\hat{\alpha} : [t_0, \infty) \rightarrow \mathbb{R}_{\geq 0}$ is a monotonically increasing function and it converges thus to some constant positive value $\hat{\alpha}^* > 0$, since $\hat{\alpha}(t_0) \geq 0$ and $\lim_{t \rightarrow \infty} \hat{\alpha}(t) = \lim_{t \rightarrow \infty} \tilde{\alpha}(t) = 0$. Therefore, we conclude that the system will converge to an equilibrium $s^* := [(x^*)^\top, 0_n^\top, 0, \hat{\alpha}^*]$ satisfying $\nabla_x \phi(x)|_{x^*} = 0$. Since $\lim_{t \rightarrow \infty} \nabla_x \phi(x)|_{x(t)} = \lim_{t \rightarrow \infty} v(t) = 0$, the system converges to the critical points of $\phi(x)$, i.e., we

obtain from (9) that at steady state:

$$2k_1(x^* - x_d) = -k_2 \sum_{j \in \bar{\mathcal{J}}} \beta'(d_j^*)(x^* - c_j), \quad (15)$$

where $d_j^* := d_j(x^*)$, $\forall j \in \bar{\mathcal{J}}$. According to the choice of τ in Prop. 1, $x^* = x_d$ implies that $\beta'(d_j^*) = 0$, $\forall j \in \bar{\mathcal{J}}$, and hence the desired equilibrium $x^* = x_d$ satisfies (15). Other undesired critical points of $\phi(x)$ consist of cases where the two sides of (15) cancel each other out. However, as already proved, only one β'_j can be nonzero for each $x \in \mathcal{F}$. Hence, the undesired critical points satisfy one of the following expressions:

$$k_1(x^* - x_d) = -k_2\beta'(d_k^*)(x^* - c_k), \quad (16a)$$

$$k_1(x^* - x_d) = k_2\beta'(d_0^*)x^*, \quad (16b)$$

for some $k \in \bar{\mathcal{J}}$. In the case of (16b), x^* is collinear with the origin and x_d . However, the choice of $\tau < \bar{r}_{\mathcal{W}}^2 - \|x_d\|^2$ in Prop. 1 implies that

$$d_0^* = \bar{r}_{\mathcal{W}}^2 - \|x^*\|^2 \leq \tau < \bar{r}_{\mathcal{W}}^2 - \|x_d\|^2 \Leftrightarrow \|x^*\| \geq \|x_d\|,$$

and hence $x^* - x_d$ and x^* have the same direction. Therefore, since $\beta'(d_j) < 0$, for $d_j < \tau$, $\forall j \in \bar{\mathcal{J}}$, (16b) is not feasible.

Moreover, in the case of (16a), since $\beta' \leq 0$, $x^* - x_d$ and $x^* - c_k$ point to the same direction. Hence, the respective critical points x^* are on the 1D line connecting x_d and c_k . Moreover, since $\tau < \bar{r}_d \leq \|x_d - c_k\|^2 - \bar{r}_{o_k}^2$, as chosen in Prop. 1, it holds that

$$\begin{aligned} d_k^* = \|x^* - c_k\|^2 - \bar{r}_{o_k}^2 &< \|x_d - c_k\|^2 - \bar{r}_{o_k}^2 \Leftrightarrow \\ \|x^* - x_d\| &> \|x^* - c_k\|. \end{aligned}$$

We proceed now by showing that the critical points satisfying (16a) are saddle points, which have a lower dimension stable manifold. Consider, therefore, the error $e_x = x - x^*$, where $x^* \neq x_d$ represents the potential undesired equilibrium point that satisfies (16a). Let also $s_e := [s_x^\top, \tilde{\alpha}^\top]^\top$, where $s_x := [e_x^\top, v^\top, \tilde{m}^\top]^\top$, whose linearization around zero yields, after using (14) and $\left. \frac{\partial f(x,v)}{\partial x} \right|_{v=0_n} = 0_{n \times n}$,

$$\dot{s}_e = \bar{A}_s s_e, \quad (17)$$

where

$$\bar{A}_s := \begin{bmatrix} A_s & 0_{2n+2} \\ 0_{2n+2}^\top & 0 \end{bmatrix}, A_s := \begin{bmatrix} 0_{n \times n} & I_n & 0_n \\ A_{s,21} & A_{s,22} & g \\ A_{s,31} & -k_m g^\top & 0 \end{bmatrix}, \quad (18)$$

and

$$A_{s,21} := -\frac{1}{m} (k_\phi + k_v + \hat{\alpha}^*) \nabla_x^2 \phi(x) \Big|_{x^*}$$

$$A_{s,22} := -\nabla_x^2 \phi(x) \Big|_{x^*} - (k_v + \hat{\alpha}^*) I_n - \frac{\partial f(x, v)}{\partial v} \Big|_{s^*}.$$

We aim to prove that the equilibrium $s_x^* := [0_n^\top, 0_n^\top, 0]^\top$ has at least one positive eigenvalue. To this end, consider a vector $\bar{\nu} := [\mu\nu^\top, \nu^\top, 0]^\top$, where $\mu > 0$ is a positive constant, and $\nu \in \mathbb{R}^n$ is an orthogonal vector to $(x^* - c_k)$, i.e. $\nu^\top (x^* - c_k) = 0$. Then the respective quadratic form yields

$$\bar{\nu}^\top A_s \bar{\nu} = \begin{bmatrix} \nu^\top A_{s,21} & \mu\nu^\top + \nu^\top A_{s,22} & \nu^\top g \end{bmatrix} \begin{bmatrix} \mu\nu \\ \nu \\ 0 \end{bmatrix} =$$

$$\mu\nu^\top A_{s,21} \nu + \mu\|\nu\|^2 + \nu^\top A_{s,22} \nu,$$

which, after employing (9) with $\beta'(d_j^*) = 0, \forall j \in \mathcal{J} \setminus \{k\}$ and $\nu^\top (x^* - c_k) = 0$, becomes

$$\bar{\nu}^\top A_s \bar{\nu} = -\frac{2\mu k_1}{m} \left(k_\phi + k_v + \frac{3}{2} \hat{\alpha}^* \right) \left(1 + \frac{k_2}{k_1} \beta'(d_k^*) \right) \|\nu\|^2$$

$$+ \mu\|\nu\|^2 - 2k_1 \left(1 + \frac{k_2}{k_1} \beta'(d_k^*) \right) \|\nu\|^2 - \left(k_v + \frac{3}{2} \hat{\alpha}^* \right) \|\nu\|^2 - \nu^\top \frac{\partial f(x, v)}{\partial v} \Big|_{s^*} \nu.$$

From (16a), by recalling that $\beta'(d_k) \leq 0$, we obtain that

$$\frac{k_2}{k_1} \beta'(d_k^*) = -\frac{\|x^* - x_d\|}{\|x^* - c_k\|} < -1. \quad (19)$$

Therefore by defining $c^* := -\frac{k_2}{k_1} \beta'(d_k^*) - 1 > 0$, we obtain

$$\bar{\nu}^\top A_s \bar{\nu} = \left(\frac{2\mu k_1}{m} k_\phi c^* + \left(\frac{2\mu k_1}{m} c^* - 1 \right) \left(k_v + \frac{3}{2} \hat{\alpha}^* \right) + \mu + 2k_1 c^* \right) \|\nu\|^2$$

$$- \nu^\top \frac{\partial f(x, v)}{\partial v} \Big|_{s^*} \nu,$$

which is rendered positive by choosing a sufficiently large μ . Hence, A_s has at least one positive eigenvalue. Next, we prove that A_s has no zero eigenvalues by proving that its determinant is nonzero. For the determinant of $\nabla_x^2 \phi(x)|_{x^*}$, in view of (9) that

$$\det(\nabla_x^2 \phi(x)|_{x^*}) = \det \left(2(k_1 + k_2 \beta'(d_k^*)) I_n + 2k_2 \beta''(d_k^*)(x^* - c_k)(x^* - c_k)^\top \right).$$

By using the property $\det(A + uv^\top) = (1 + v^\top A^{-1}u) \det(A)$, for any invertible matrix A and vectors u, v , we obtain

$$\det(\nabla_x^2 \phi(x)|_{x^*}) = 2^n (k_1 + k_2 \beta'(d_k^*))^n \left(1 + \frac{k_2}{k_1 \left(1 + \frac{k_2}{k_1} \beta'(d_k^*) \right)} \beta''(d_k^*) \|x^* - c_k\|^2 \right). \quad (20)$$

In view of (19) and by using $\|x^* - x_d\| - \|x^* - c_k\| = \|x_d - c_k\|$ since x^*, c_k and x_d are collinear, (20) becomes

$$\det(\nabla_x^2 \phi(x)|_{x^*}) = 2^n (k_1 k_2 \beta'(d_k^*))^n \left(1 - \frac{k_2}{k_1 \|x_d - c_k\|} \beta''(d_k^*) \|x^* - c_k\|^3 \right).$$

Note that, since $\lim_{d_j \rightarrow 0} \beta(d_j) = \infty$ and $\beta(d_j)$ decreases to $\beta(d_j) = \beta(\tau)$, $\forall d_j \geq \tau$, the derivatives $\beta'(d_j)$ satisfy $\lim_{d_j \rightarrow 0} \beta'(d_j) = -\infty$ and increase to $\beta'(d_j) = 0$, $\forall d_j \geq \tau$. Hence, we conclude that $\beta''(d_j) > 0$, $\forall d_j \in (0, \tau)$. Therefore, in order for the critical point to be non-degenerate, we must guarantee that

$$\frac{k_2}{k_1 \|x_d - c_k\|} \beta''(d_k^*) \|x^* - c_k\|^3 > 1. \quad (21)$$

By expressing $\|x^* - c_k\|^3 = (d_k^* + \bar{r}_{o_k}^2) \sqrt{d_k^* + \bar{r}_{o_k}^2}$, considering that $\|x_d - c_k\| \leq 2\bar{r}_{\mathcal{W}}$ and setting $\underline{r} := \min_{j \in \mathcal{J}} \{\bar{r}_{o_j}\}$, a lower bound for the left-hand side of (21) is

$$f_\ell(d_k^*) := \frac{k_2}{2k_1 \bar{r}_{\mathcal{W}}} \beta''(d_k^*) (d_k(x^*) + \underline{r}^2) \sqrt{d_k(x^*) + \underline{r}^2}. \quad (22)$$

According to Property 4 of Definition 1, (22) is a decreasing function of d_k^* , for $d_k^* \in (0, \tau)$, with $f_\ell(\tau) = 0$ and $\lim_{d_k^* \rightarrow 0} f_\ell(d_k^*) = \infty$. Therefore, there

exists a positive $d_k^{\star\star} > 0$, such that $f_\ell(d_k^{\star}) > 1$, $\forall d_k^{\star} < d_k^{\star\star}$. Hence, by setting $\tau < d_k^{\star\star}$, we achieve $d_k^{\star} < \tau < d_k^{\star\star}$ and guarantee that $f_\ell(d_k^{\star}) > 1$.

By defining $A_{2ns} := \begin{bmatrix} 0_{n \times n} & I_n \\ A_{s,21} & A_{s,22} \end{bmatrix}$, it holds that

$$\det(A_{2ns}) = \det(A_{s,21}) = \frac{(-1)^n}{m^n} \left(k_\phi + k_v + \frac{3}{2} \hat{\alpha}^{\star} \right)^n \det(\nabla_x^2 \phi(x)|_{x^{\star}}) \neq 0.$$

Moreover, it holds that $A_{2ns}^{-1} = \begin{bmatrix} \star & A_{s,21}^{-1} \\ \star & 0_{n \times n} \end{bmatrix}$ and therefore we obtain that

$$\begin{aligned} \det(A_s) &= \det(A_{s,21}) \begin{bmatrix} k_m g^\top (\nabla_x^2 \phi(x))^\top|_{x^{\star}} & k_m g^\top \end{bmatrix} A_{2ns}^{-1} \begin{bmatrix} 0_n \\ g \end{bmatrix} \\ &= \det(A_{s,21}) \begin{bmatrix} k_m g^\top (\nabla_x^2 \phi(x))^\top|_{x^{\star}} & k_m g^\top \end{bmatrix} \begin{bmatrix} A_{s,21}^{-1} & g \\ 0_n & \end{bmatrix} \\ &= \det(A_{s,21}) k_m g^\top (\nabla_x^2 \phi(x))^\top|_{x^{\star}} A_{s,21}^{-1} g \\ &= k_m g^\top (\nabla_x^2 \phi(x))^\top|_{x^{\star}} \text{adj}(A_{s,21}) g, \end{aligned}$$

which is non-zero, since

$$\det(\nabla_x^2(\phi(x))^\top|_{x^{\star}} \text{adj}(A_{s,21})) = \det(\nabla_x^2(\phi(x))^\top|_{x^{\star}}) \det(A_{s,21})^{n-1} \neq 0,$$

and $g \neq 0_n$ ², and hence the matrix that forms the latter quadratic form is nonsingular.

Therefore, we conclude that A_s is non-degenerate and has at least one positive eigenvalue. Note that \bar{A}_s has the same eigenvalues as A_s and an extra zero eigenvalue. According to the Reduction Principle [40, Th. 5.2], $\dot{s}_e = \bar{A}_s s_e$ is locally topologically equivalent near the origin to the system

$$\begin{aligned} \dot{\hat{\alpha}} &= k_\alpha \|v_\alpha(\hat{\alpha}) + \nabla_x \phi(x)|_{x_\alpha(\hat{\alpha})}\|^2 \\ \dot{s}_x &= A_s s_x, \end{aligned}$$

where $v_\alpha(\hat{\alpha})$, $\nabla_x \phi(x)|_{x_\alpha(\hat{\alpha})}$ are the restrictions of v and $\nabla_x \phi(x)$ to the center manifold of $\hat{\alpha}$ [40, Theorem 5.2]. Regarding the trajectories of s_x , since A_s is a non-degenerate saddle (it has at least one positive eigenvalue) its stable manifold has dimension lower than $2n + 1$ and is thus a set of zero measure. Therefore, all the initial conditions $(x(t_0), v(t_0), \tilde{m}(t_0)) \in \mathcal{F} \times \mathbb{R}^{n+1}$, except for the aforementioned lower-dimensional manifold, converge to the desired equilibrium $(x_d, 0_n, 0)$.

²A similar analysis can be performed in the 2-dimensional, where $g = 0_n$.

Remark 1 *Note that, unlike the related works in feedback-based robot navigation, the proposed algorithm guarantees almost global safe convergence while compensating for unknown dynamic terms (f and m in this case). Moreover, in contrast to tuning schemes (e.g., [3, 6, 14, 33]), we do not require large control gains in order to establish the correctness of the propose scheme.*

Remark 2 *The condition $k_\phi > \frac{\alpha}{2}$ of Theorem 1 is only sufficient and not necessary, as will be shown in the simulation results. Moreover, in case the robot gets stuck in a local minima, one could apply an exciting input perpendicular to $x - x_d$ (see [17]), freeing it thus from that configuration. Nevertheless, the set of initial conditions that drive the robot to such configurations has zero measure and hence the probability of starting in it is zero.³*

4.1 Dynamic Disturbance Addition

Except for the already considered dynamic uncertainties, we can add to the right-hand side of (1) an unknown disturbance vector $d(x, v, t)$, i.e.,

$$\begin{aligned}\dot{x} &= v \\ m\dot{v} + f(x, v) + mg + d(x, v, t) &= u,\end{aligned}$$

subject to a uniform boundedness condition $\|d(x, v, t)\| \leq \bar{d}$, $\forall x, v, t \in \mathbb{R}^{2n} \times \mathbb{R}_{\geq 0}$. In this case, by slightly modifying the control scheme, we still guarantee collision avoidance with the workspace obstacles and boundary. In addition, we achieve uniform ultimate boundedness of the error signals as well as the gradient of ϕ , as the analysis in this section shows.

The control scheme of the previous section is appropriately enhanced to incorporate the σ -modification [39], a common technique in adaptive control. More specifically, the adaptation laws (12) are modified according to

$$\begin{aligned}\dot{\hat{m}} &:= -k_m e_v^\top (\dot{v}_d + g) - \sigma_m \hat{m} \\ \dot{\hat{\alpha}} &:= k_\alpha \|e_v\|^2 - \sigma_\alpha \hat{\alpha},\end{aligned}$$

where σ_m, σ_α are positive gain constants, to be appropriately tuned as per the analysis below.

³The exciting input could be applied at the initial condition, if it can be identified that it will lead to a local minima.

Consider now the function V as defined (13). In view of the analysis of the previous section, the incorporation of $d(x, v, t)$, as well as the modification of the adaptation laws, the derivative of V becomes

$$\begin{aligned}\dot{V} \leq & -\left(k_\phi - \frac{\alpha}{2}\right)\|\nabla_x \phi(x)\|^2 - k_v \|e_v\|^2 + \|e_v\| \bar{d} \\ & - \frac{3}{2}\sigma_\alpha \tilde{\alpha} \hat{\alpha} - \sigma_m \tilde{m} \hat{m},\end{aligned}$$

which, by using $\hat{\alpha} = \tilde{\alpha} + \alpha$, $\hat{m} = \tilde{m} + m$, as well as the properties $-ab = -\frac{1}{2}(a+b)^2 + \frac{a^2}{2} + \frac{b^2}{2}$, $ab = -\frac{1}{2}(a-b)^2 + \frac{a^2}{2} + \frac{b^2}{2}$, $\forall a, b \in \mathbb{R}$, becomes

$$\begin{aligned}\dot{V} \leq & -\left(k_\phi - \frac{\alpha}{2}\right)\|\nabla_x \phi(x)\|^2 - \left(k_v - \frac{1}{2}\right)\|e_v\|^2 + \frac{\bar{d}^2}{2} - 3\sigma_\alpha \frac{\tilde{\alpha}^2}{4} \\ & - \sigma_m \frac{\tilde{m}^2}{2} + 3\sigma_\alpha \frac{\alpha^2}{4} + \sigma_m \frac{m^2}{2} \leq -k_\xi \|\xi\|^2 + d_\xi,\end{aligned}$$

where $\xi := [\nabla_x \phi(x)^\top, e_v^\top, \tilde{m}, \tilde{\alpha}]^\top \in \mathbb{R}^{2n+2}$, $k_\xi := \min\{k_\phi - \frac{\alpha}{2}, k_v - \frac{1}{2}, \frac{\sigma_m}{2}, \frac{3\sigma_\alpha}{4}\}$, and $d_\xi := \frac{\bar{d}^2}{2} + 3\sigma_\alpha \frac{\alpha^2}{4} + \sigma_m \frac{m^2}{2}$. Therefore, \dot{V} is negative when $\|\xi\| > \sqrt{\frac{d_\xi}{k_\xi}}$, which, by also requiring $k_v > \frac{1}{2}$, implies that

$$\|\xi(t)\| \leq \max \left\{ \gamma_1(\|\xi(t_0)\|), \gamma_2 \left(\sqrt{\frac{d_\xi}{k_\xi}} \right) \right\},$$

$\forall t \geq t_0$, where γ_i are class K functions [41, Th. 4.18]. Since $\xi(t)$, and hence $\nabla_x \phi(x)$, remain bounded, collisions are avoided.

Note that the aforementioned analysis guarantees that $\nabla_x \phi(x)|_{x(t)}$ will be ultimately bounded in a set close to zero. This point, however, might be a critical point of ϕ and it is not guaranteed that $x(t)$ will be bounded close to the goal configuration x_d . Nevertheless, intuition suggests that if the disturbance vector $d(x, v, t)$ does not behave adversarially, the agent will converge close to the goal configuration. This is also verified by the simulation results of Section 7.

5 Extension to Star Worlds

In this section, we discuss how the proposed control scheme can be extended to generalized sphere worlds, and in particular *star worlds*, being inspired by the methodology of [4]. That work however, like others related to workspace transformations [14, 16], consider simplified dynamics without taking into

account unknown terms, which is the focus of this section. Although we focus on star-worlds, the analysis holds for any diffeomorphic transformation that exhibits the desired properties (e.g. [14]). *Star worlds* are diffeomorphic to sphere worlds sets of the form $\mathcal{T} := \bar{\mathcal{W}} \setminus \bigcup_{j \in \mathcal{J}} \bar{O}_{\mathcal{T}_j}$, where $\bar{\mathcal{W}}$ is a workspace of the form (4) and $\bar{O}_{\mathcal{T}_j}$ are M disjoint star-shaped obstacles (indexed by $\mathcal{J} = \{1, \dots, M\}$). The latter are sets characterized by the property that all rays emanating from a center point cross their boundary only once [4]. One can design a diffeomorphic mapping $H : \mathcal{T} \rightarrow \mathcal{F}$, where \mathcal{F} is a sphere world of the type (5). More specifically, H maps the boundary of \mathcal{T} to the boundary of \mathcal{F} . Construction of such a mapping is beyond the scope of the paper and we refer the interested reader to the related literature [4, 42].

The control scheme of the previous section is modified now to account for the transformation H as follows. The desired robot velocity is set to $v_d : \mathcal{T} \rightarrow \mathbb{R}^n$, with

$$v_d(x) := -J_H(x)^{-1} \nabla_{H(x)} \phi(H(x)), \quad (23)$$

where $J_H(x) := \frac{\partial H(x)}{\partial x}$ is the nonsingular Jacobian matrix of H . Next, by letting $e_v := v - v_d$, the control law is designed as $u : \mathcal{T} \times \mathbb{R}^{n+2} \rightarrow \mathbb{R}^n$, with

$$u := u(x, v, \hat{m}, \hat{\alpha}) := -k_\phi J_h(x)^\top \nabla_{H(x)} \phi(H(x)) + \hat{m}(\dot{v}_d + g) - \left(k_v + \frac{3}{2}\hat{\alpha}\right) e_v, \quad (24)$$

where \hat{m} and $\hat{\alpha}$ evolve according to the respective expressions in (12). The next theorem gives the main result of this section.

Theorem 2 *Consider a robot operating in \mathcal{W} , subject to the uncertain 2nd-order dynamics (1). Given $x_d \in \mathcal{T}$, the control protocol (23), (24), (12) guarantees the collision-free navigation to x_d from almost all initial conditions $(x(t_0), v(t_0), \hat{m}(t_0), \hat{\alpha}(t_0)) \in \mathcal{T} \times \mathbb{R}^{n_1} \times \mathbb{R}_{\geq 0}$, given a sufficiently small τ and that $k_\phi > \frac{\alpha}{2}$. Moreover, all closed loop signals remain bounded, $\forall t \geq t_0$.*

Proof *Following similar steps as in the proof of Theorem 1, we consider the function*

$$V := k_\phi \phi(H(x)) + \frac{m}{2} \|e_v\|^2 + \frac{1}{2k_\alpha} \tilde{\alpha}^2 + \frac{1}{2k_m} \tilde{m}^2, \quad (25)$$

whose derivative along the solutions of the closed loop system yields

$$\dot{V} \leq -\left(k_\phi - \frac{\alpha}{2}\right) \|\nabla_{H(x)} \phi(H(x))\|^2 - k_v \|e_v\|^2 \leq 0, \quad (26)$$

which proves the boundedness of the obstacle functions $\beta(d_j(H(x(t))))$, $\forall j \in \mathcal{J}, t \geq t_0$. Since the boundaries $\partial\bar{\mathcal{O}}_j$ are mapped to $\partial\bar{\mathcal{O}}_{\mathcal{T}_j}$ through $H(x)$, we conclude that $x(t) \in \mathcal{T}$, $t \geq t_0$ and no collisions occur. Next, by following similar arguments as in the proof of Theorem 1, we conclude that the solution will converge to a critical point of $\phi(H(x))$. By choosing a sufficiently small τ for the obstacle functions $\beta(d_j(H(x(t))))$, the critical points consist of the desired equilibrium, where $\beta'(d_j(H(x_d))) = 0$, $\forall j \in \mathcal{J}$, or undesired critical points x^* satisfying

$$k_1(H(x^*) - H(x_d)) = -k_2\beta'(d_{H_k}^*)(H(x^*) - H(c_k)), \quad (27)$$

for some $k \in \mathcal{J}$, where we define $d_{H_j}^* := d_j(H(x^*))$, $\forall j \in \mathcal{J}$. The respective terms of the linearization matrix \bar{A}_s from (17) become now

$$\bar{A}_s := \begin{bmatrix} A_s & 0_{2n+2} \\ 0_{2n+2}^\top & 0 \end{bmatrix}$$

$$A_s := \begin{bmatrix} 0_{n \times n} & I_n & 0_n \\ A_{s,21} & A_{s,22} & g \\ A_{s,31} & -k_m g^\top & 0 \end{bmatrix},$$

with

$$A_{s,21} := -\frac{1}{m}(k_\phi J_H(x^*)^\top + \left(k_v + \frac{3}{2}\hat{\alpha}^*\right) J_H(x^*)^{-1}) \nabla^2 \phi^* J_H(x^*)$$

$$A_{s,22} := -J_H(x^*)^{-1} \nabla^2 \phi^* J_H(x^*) - \left(k_v + \frac{3}{2}\hat{\alpha}^*\right) I_n - \frac{\partial f(x, v)}{\partial v} \Big|_{s^*},$$

$$A_{s,31} := -k_m g^\top (J_H(x^*)^{-1} \nabla^2 \phi^* J_H(x^*))^\top$$

and $\nabla^2 \phi^* := \nabla_{H(x)}^2 \phi(H(x))|_{x^*}$, around $x = x^*, v = 0, \tilde{m} = 0, \tilde{\alpha} = \tilde{\alpha}^*$. Next, similarly to the proof of Theorem 2, we prove that $\bar{v}^\top A_s \bar{v} > 0$, for $\bar{v} := [\mu \nu^\top, \nu^\top, 0]^\top$, where $\mu > 0$ is a positive constant and $\nu := J_H(x^*)^{-1} \hat{\nu}$, with $\hat{\nu} \in \mathbb{R}^n$ a vector orthogonal to $(H(x^*) - H(c_k))$. The respective quadratic form yields, after employing (27) and defining $c^* := -\left(1 + \frac{k_2}{k_1} \beta'(d_{H_k}^*)\right) > 0$:

$$\bar{v}^\top A_s \bar{v} = \hat{\nu}^\top \left[\frac{2k_1 k_\phi \mu c^*}{m} I_n + J_H(x)^{-\top} \left(\left(\frac{2k_1 c^* (k_v + \frac{3}{2}\hat{\alpha}^*)}{m} + \mu - \left(k_v + \frac{3}{2}\hat{\alpha}^* \right) + 2k_1 c^* \right) I_n - \frac{\partial f(x, v)}{\partial v} \Big|_{s^*} \right) J_H(x)^{-1} \right] \hat{\nu},$$

which can be rendered positive for sufficiently large μ .

Moreover, at a critical point $x^{\star,1}$ of $\phi(H(x))$, it holds that (see the proof of Prop. 2.6 in [3]),

$$\nabla_{H(x)}^2 \phi(H(x))|_{x^{\star,1}} = J_H(x^{\star,1})^\top \nabla_x^2 \phi(x)|_{x^{\star,2}} J_H(x^{\star,1}),$$

where $x^{\star,2}$ is a critical point of $\phi(x)$ satisfying $x^{\star,2} = H(x^{\star,1})$. Since $J_H(x)$ is nonsingular, it holds that $x^{\star,1}$ is non-degenerate if and only if $x^{\star,2}$ is non-degenerate. As already shown in the proof of Theorem 1, by choosing τ sufficiently small, we render the critical points of $\phi(x)$ that are close to the obstacles non-degenerate. Hence, we conclude that the respective critical points of $\phi(H(x))$ are also non-degenerate and $\det(\nabla^2 \phi^\star) \neq 0$.

Next, in order to prove that the critical point $(x^\star, 0, 0)$ is non-degenerate, we calculate the determinant of A_s . Following the proof of Theorem 1, we obtain that

$$\begin{aligned} \det(A_s) &= \det(A_{s,21}) k_m g^\top (J_H(x^\star)^{-1} \nabla^2 \phi^\star J_H(x^\star))^\top A_{s,21}^{-1} g \\ &= k_m g^\top (J_H(x^\star)^{-1} \nabla^2 \phi^\star J_H(x^\star))^\top \text{adj}(A_{s,21}) g \end{aligned}$$

where

$$\begin{aligned} \det(A_{s,21}) &= (-1)^n \left(\frac{k_\phi^n}{m^n} \det(J_H(x^\star)) + \right. \\ &\quad \left. \left(k_v + \frac{3}{2} \hat{\alpha}^\star \right)^n \frac{1}{\det(J_H(x^\star))} \right) \det(\nabla^2 \phi^\star) \det(J_H(x^\star)), \end{aligned}$$

which is not zero, since $\det(\nabla^2 \phi^\star) \neq 0$ and $J_H(x^\star) \neq 0$. Hence, we conclude that the aforementioned quadratic form is also not zero and hence the non-degeneracy of the critical points under consideration. Hence, by following similar arguments as in the proof of Theorem 1, we conclude that the initial conditions that converge to these critical saddle points form a set of measure zero.

Remark 3 The proposed schemes can also be extended to unknown environments, where the amount and location of the obstacles is unknown a priori, and these are sensed locally on-line. In particular, by having a large enough sensing neighborhood, each obstacle $j \in \mathcal{J}$ can be sensed when $d_j = \tau$, and hence the respective term can be smoothly incorporated in $\nabla_x \phi(x)$, in view

of the properties of β (a similar idea is discussed in Section V of [10]). It should be noted, however, that the local sensory information and respective hardware must allow for the accurate estimation of the centers and radii (or the implicit function in case of star-worlds) of the obstacles.

6 Extension to Multi-Robot Systems

This section is devoted to extending the results of Section 4 to multi-robot systems. Consider, therefore, $N \in \mathbb{N}$ spherical robots operating in a workspace \mathcal{W} of the form (3), characterized by their position vectors $x_i \in \mathbb{R}^n$, as well as their radii $r_i > 0$, $i \in \mathcal{N} := \{1, \dots, N\}$, and obeying the second-order uncertain dynamics (1), i.e.,

$$\dot{x}_i = v_i \tag{28a}$$

$$m_i \dot{v}_i + f_i(x_i, v_i) + m_i g = u_i, \tag{28b}$$

with the unknown $f_i(\cdot)$ satisfying $\|f_i(x_i, v_i)\| \leq \alpha_i \|v_i\|$, for unknown positive constants α_i , $\forall i \in \mathcal{N}$. We also denote $x := [x_1^\top, \dots, x_N^\top]^\top$, $v := [v_1^\top, \dots, v_N^\top]^\top \in \mathbb{R}^{Nn}$. Each robot's destination is x_{d_i} , $i \in \mathcal{N}$.

The proposed multi-robot scheme is based on a prioritized leader-follower coordination. Prioritization in multi-agent systems for navigation-type objectives has been employed in [9] and [43], where KRNf gain tuning-type methodologies are developed. The proposed framework, however, is substantially different from these works; [43] does not take into account inter-agent collisions, and uses prioritization for the sequential navigation and task satisfaction subject to connectivity constraints, while [9] uses prioritization for directional collision-avoidance. In our proposed prioritized leader-follower methodology, the leader robot, by appropriately choosing the offset τ , “sees” the other robots as static obstacles and hence the overall scheme reduces to the one of Section 4. This is accomplished by differentiating the free spaces of the leader and the followers. Moreover, the aforementioned works [9, 43] consider simplified first-order dynamics and cannot be easily extended to the uncertain dynamics-case considered here. In fact, we note that, according to our best knowledge, there does not exist a control framework that provably guarantees decentralized safe multi-robot navigation in workspaces with obstacles and subject to uncertain 2nd-order dynamics.

The workspace is assumed to satisfy Assumption 2 and we further impose the following extra conditions:

Assumption 3 *The workspace \mathcal{W} , obstacles \mathcal{O}_j , $j \in \mathcal{J}$, and destinations x_{d_i} , $i \in \mathcal{N}$, satisfy:*

$$\begin{aligned} \|c_j - x_{d_i}\| &> r_{o_j} + r_i + 2r_M + \varepsilon, \forall i, j \in \mathcal{N} \times \mathcal{J} \\ \|x_{d_i} - x_{d_j}\| &> r_i + r_j + 2r_M + 2\varepsilon, \forall i, j \in \mathcal{N}, i \neq j \\ r_{\mathcal{W}} - \|x_{d_i}\| &> r_i + 2r_M + \varepsilon, \forall i \in \mathcal{N} \end{aligned}$$

whereas the initial positions satisfy:

$$\begin{aligned} \|c_j - x_i(t_0)\| &> r_{o_j} + r_i + 2r_M, \forall i, j \in \mathcal{N} \times \mathcal{J} \\ r_{\mathcal{W}} - \|x_i(t_0)\| &> r_i + 2r_M, \forall i \in \mathcal{N} \\ \|x_{d_i} - x_j(t_0)\| &> r_i + r_j + 2r_M + \varepsilon, \forall i, j \in \mathcal{N}, i \neq j, \end{aligned}$$

for an arbitrarily small positive constant ε , $\forall i \in \mathcal{N}, j \in \mathcal{J}$, where $r_M := \max_{i \in \mathcal{N}} \{r_i\}$.

Loosely speaking, the aforementioned assumption states that the pair-wise distances among obstacles, workspace boundary, initial conditions and final destinations are large enough so that one robot can always navigate between them. Since the convergence of the agents to the their destinations is asymptotic, we incorporate the threshold ε , which is the desired proximity we want to achieve to the destination, as will be clarified in the sequel. Intuitively, since we cannot achieve $x_i = x_{d_i}$ in finite time, the high-priority agents will stop once $\|x_i - x_{d_i}\| = \varepsilon$, which is included in the aforementioned conditions to guarantee the feasibility of the collision-free navigation for the lower-priority agents. Similarly to the single-agent case, we can find a positive constant \bar{r} such that (6) hold as well as

$$\|c_j - x_i(t_0)\| > r_{o_j} + r_i + 2r_M + 2\bar{r}, \forall i, j \in \mathcal{N} \times \mathcal{J} \quad (29a)$$

$$r_{\mathcal{W}} - \|x_i(t_0)\| > r_i + 2r_M + 2\bar{r}, \forall i \in \mathcal{N} \quad (29b)$$

$$\|c_j - x_{d_i}\| > r_{o_j} + r_i + 2r_M + \varepsilon + 2\bar{r}, \forall i, j \in \mathcal{N} \times \mathcal{J} \quad (29c)$$

$$\|x_{d_i} - x_{d_j}\| > r_i + r_j + 2r_M + 2\varepsilon + 2\bar{r}, \forall i, j \in \mathcal{N}, i \neq j \quad (29d)$$

$$\|x_{d_i} - x_j(t_0)\| > r_i + r_j + 2r_M + \varepsilon + 2\bar{r}, \forall i, j \in \mathcal{N}, i \neq j \quad (29e)$$

$$r_{\mathcal{W}} - \|x_{d_i}\| > r_i + 2r_M + \varepsilon + 2\bar{r}, \forall i \in \mathcal{N} \quad (29f)$$

We consider that the agents have a limited sensing range, defined by a radius $\varsigma_i > 0$, $i \in \mathcal{N}$, and we assume that each agent i can sense the state of its neighbors:

Assumption 4 Each agent $i \in \mathcal{N}$ has a limited sensing radius ς_i , satisfying $\varsigma_i > \sqrt{\min(\bar{r}^2, \bar{r}_d)} + r_i + r_j + 2r_M + 2\bar{r}$, with \bar{r}_d as defined in (7), and has access to $x_i - x_j, v_i - v_j, \forall j \in \{j \in \mathcal{N} : \|x_i - x_j\| \leq \varsigma_i\}$.

Moreover, we consider that the destinations, $x_{d_i}, i \in \mathcal{N}$, as well as the radii, r_i , are transmitted off-line to all the agents⁴. Consider now a prioritization of the agents, possibly based on some desired metric (e.g., distance to their destinations), which can be performed off-line and transmitted to all the agents. Our proposed scheme is based on the following algorithm. The agent with the highest priority is designated as the leader of the multi-agent system, indexed by $i_{\mathcal{L}}$, whereas the rest of the agents are considered as the followers, defined by the set $\mathcal{N}_{\mathcal{F}} := \mathcal{N} \setminus \{i_{\mathcal{L}}\}$. The followers and leader employ a control protocol that has the same structure as the one of Section 4. The key difference here lies in the definition of the free space for followers and leaders. Let $q = [q_1^\top, \dots, q_N^\top]^\top \in \mathbb{R}^{Nn}$. We define first the sets

$$\begin{aligned}\bar{\mathcal{W}}_{i_{\mathcal{L}}} &:= \{q \in \mathbb{R}^{Nn} : \|q_{i_{\mathcal{L}}}\| < r_{\mathcal{W}} - r_{i_{\mathcal{L}}}\}, \\ \bar{\mathcal{O}}_{i_{\mathcal{L}},j} &:= \{q \in \bar{\mathcal{W}}_{i_{\mathcal{L}}} : \|q_i - c_j\| \leq r_{o_j} + r_i\}, \forall j \in \mathcal{J} \\ \mathcal{C}_{i_{\mathcal{L}}} &:= \{q \in \bar{\mathcal{W}}_{i_{\mathcal{L}}} : \|q_{i_{\mathcal{L}}} - q_j\| \leq r_{i_{\mathcal{L}}} + r_j, \forall j \in \mathcal{N} \setminus \{i_{\mathcal{L}}\}\},\end{aligned}$$

which correspond to the leader agent, as well as the follower sets

$$\begin{aligned}\bar{\mathcal{W}}_i &:= \{q \in \mathbb{R}^{Nn} : \|q_i\| < r_{\mathcal{W}} - r_i - 2r_M - 2\bar{r}\} \\ \bar{\mathcal{O}}_{i,j} &:= \{q \in \bar{\mathcal{W}}_i : \|q_i - c_j\| \leq r_{o_j} + r_i + 2r_M + 2\bar{r}\}, \forall j \in \mathcal{J} \\ \mathcal{C}_i &:= \{q \in \bar{\mathcal{W}}_i : \|q_i - q_{i_{\mathcal{L}}}\| \leq r_i + r_{i_{\mathcal{L}}}, \\ &\quad \|q_i - q_j\| \leq r_i + r_j + 2r_M + 2\bar{r}, \forall j \in \mathcal{N} \setminus \{i_{\mathcal{L}}, i\}, \\ &\quad \|q_i - x_{d_j}\| \leq r_i + r_j + 2r_M + 2\bar{r} + \varepsilon, \forall j \in \mathcal{N}_i\},\end{aligned}$$

$\forall i \in \mathcal{N}_{\mathcal{F}}$, where \mathcal{N}_i denotes the set of agents with higher priority than agent i . The free space for the agents is defined then as $\mathcal{F}_i := \bar{\mathcal{W}}_i \setminus \{(\bigcup_{j \in \mathcal{J}} \bar{\mathcal{O}}_{i,j}) \cup \mathcal{C}_i\}, \forall i \in \mathcal{N}$. It can be verified that, in view of (29), the sets \mathcal{F}_i are nonempty and $x(t_0) \in \mathcal{F} := \bigcap_{i \in \mathcal{N}} \mathcal{F}_i$. The main difference lies in the fact that the follower agents aim to keep a larger distance from each other, the obstacles, and the workspace boundary than the leader agent, and in particular, a distance enhanced by $2r_M + 2\bar{r}$. In that way, the leader agent will be able to choose an appropriate constant τ (as in the single-agent case of Section 4) so that it

⁴This implies that the agents can compute r_M offline.

is influenced at each time instant only by one of the obstacles/followers, and will be also able to navigate among the obstacles/followers. Note that the followers are required to stay away also from the destinations of the higher priority agents, since a potential local minimum in such configurations can prevent the leader agent from reaching its goal. We provide next the mathematical details of the aforementioned reasoning.

Consider the leader distances $d_{i_{\mathcal{L}}, o_k}, d_{i_{\mathcal{L}}, j}, d_{i_{\mathcal{L}}, o_0} : \mathcal{F}_{i_{\mathcal{L}}} \rightarrow \mathbb{R}_{\geq 0}$ as

$$\begin{aligned} d_{i_{\mathcal{L}}, o_k}(x) &:= \|x_{i_{\mathcal{L}}} - c_k\|^2 - (r_{i_{\mathcal{L}}} + r_{o_k})^2, \forall k \in \mathcal{J} \\ d_{i_{\mathcal{L}}, j}(x) &:= \|x_{i_{\mathcal{L}}} - x_j\|^2 - (r_{i_{\mathcal{L}}} + r_j)^2, \forall j \in \mathcal{N}_{\mathcal{F}} \\ d_{i_{\mathcal{L}}, o_0}(x) &:= (r_{\mathcal{W}} + r_{i_{\mathcal{L}}})^2 - \|x_{i_{\mathcal{L}}}\|^2 \end{aligned}$$

and the follower distances $d_{i, o_k}, d_{i, i_{\mathcal{L}}}, d_{i, j}, d_{i, d_j}, d_{i, o_0} : \mathcal{F}_i \rightarrow \mathbb{R}_{\geq 0}$ as

$$\begin{aligned} d_{i, o_k}(x) &:= \|x_i - c_k\|^2 - (r_i + r_{o_k} + 2r_M + 2\bar{r})^2, \forall k \in \mathcal{J} \\ d_{i, i_{\mathcal{L}}}(x) &:= \|x_i - x_{i_{\mathcal{L}}}\|^2 - (r_i + r_{i_{\mathcal{L}}})^2 = d_{i_{\mathcal{L}}, i}(x) \\ d_{i, j}(x) &:= \|x_i - x_j\|^2 - (r_i + r_j + 2r_M + 2\bar{r})^2, \forall j \in \mathcal{N}_{\mathcal{F}} \setminus \{i\} \\ d_{i, d_j}(x) &:= \|x_i - x_{d_j}\|^2 - (r_i + r_j + 2r_M + 2\bar{r} + \varepsilon)^2, \forall j \in \mathcal{N}_i \\ d_{i, o_0}(x) &:= (r_{\mathcal{W}} - r_i - 2r_M - 2\bar{r})^2 - \|x_i\|^2, \end{aligned}$$

$\forall i \in \mathcal{N}_{\mathcal{F}}$. Note that $d_{i, j}(x) = d_{j, i}(x)$, $\forall i, j \in \mathcal{N}$, with $i \neq j$ and also that $x \in \mathcal{F}$ is equivalent to all the aforementioned distances being positive.

Let now functions $\beta, \beta_i, i \in \mathcal{N}$, that satisfy the properties of Definition 1, as well as the respective constants τ, τ_i , such that $\beta'(z) = \beta''(z) = 0, \forall z \geq \tau$, $\beta'_i(z) = \beta''_i(z) = 0, \forall z \geq \tau_i, i \in \mathcal{N}$. The 2nd-order navigation functions for the agents are now defined as $\phi_i : \mathcal{F}_i \rightarrow \mathbb{R}_{\geq 0}$, with

$$\begin{aligned} \phi_i(x) &:= k_{1_i} \|x_i - x_{d_i}\|^2 + k_{2_i} \left(b_{1_i}(x) + b_{2_i}(x) + k_{f_i} b_{3_i}(x) \right) \\ b_{1_i}(x) &:= \sum_{j \in \mathcal{J}} \beta_i(d_{i, o_j}(x)), \\ b_{2_i}(x) &:= \sum_{j \in \mathcal{N} \setminus \{i\}} \beta(d_{i, j}(x)) \\ b_{3_i}(x) &:= \sum_{j \in \mathcal{N}_i} \beta_i(d_{i, d_j}(x)), \end{aligned}$$

$\forall i \in \mathcal{N}$, and $k_{f_{i_{\mathcal{L}}}} = 0$, $k_{f_i} = 1$, $\forall i \in \mathcal{N}_{\mathcal{F}}$. Note that the robotic agents can choose independently their τ_i , $i \in \mathcal{N}$, that concerns the collision avoidance with the obstacles and the workspace boundary. The pair-wise inter-agent distances, however, are required to be the same and hence the same β (and hence τ) is chosen (see the terms $b_{2_i}(x)$ in $\phi_i(x)$), which can, nevertheless, be done off-line. To achieve convergence of the leader to its destination, we choose τ and $\tau_{i_{\mathcal{L}}}$ as in Section 4, i.e., $\tau, \tau_{i_{\mathcal{L}}} \in (0, \min\{\bar{r}^2, \bar{r}_d\})$. Regarding the ability of the agents to sense each other when $d_{i,j}(x) < \tau$, it holds that

$$\begin{aligned} d_{i,j}(x) < \tau &\Leftrightarrow \|x_i - x_j\|^2 \leq \tau + (r_i + r_j + 2r_M + 2\bar{r})^2 \Rightarrow \\ \|x_i - x_j\| &\leq \sqrt{\tau} + r_i + r_j + 2r_M + 2\bar{r} \Rightarrow \\ \|x_i - x_j\| &\leq \sqrt{\min\{\bar{r}^2, \bar{r}_d\}} + r_i + r_j + 2r_M + 2\bar{r} < \varsigma_i, \end{aligned}$$

$\forall i, j \in \mathcal{N}$, $i \neq j$, as dictated by Assumption 4.

The control protocol follows the same structure as the single-agent case presented in Section 4. In particular, we define the reference velocities as $v_{d_i} : \mathcal{F}_i \rightarrow \mathbb{R}^n$, with

$$v_{d_i}(x) := -\nabla_{x_i} \tilde{\phi}_i(x), \quad (30)$$

where $\tilde{\phi}_i : \mathcal{F}_i \rightarrow \mathbb{R}_{\geq 0}$ is the slightly modified function:

$$\tilde{\phi}_i(x) := k_{1_i} \|x_i - x_{d_i}\|^2 + k_{2_i} (b_{1_i}(x) + 2b_{2_i}(x) + k_{f_i} b_{3_i}(x))$$

The need for modification of ϕ_i to $\tilde{\phi}_i$ stems from the differentiation of the terms b_{2_i} . The control law is designed as $u_i := u_i(x, v, \hat{m}_i, \hat{\alpha}_i) : \mathcal{F}_i \times \mathbb{R}^{Nn+2} \rightarrow \mathbb{R}^n$, with

$$u_i := -k_{\phi_i} \nabla_{x_i} \tilde{\phi}_i(x) + \hat{m}_i (\dot{v}_{d_i} + g) - \left(k_{v_i} + \frac{3}{2} \hat{\alpha}_i \right) e_{v_i} \quad (31)$$

$\forall i \in \mathcal{N}$; k_{ϕ_i} , k_{v_i} are positive constants, e_{v_i} are the velocity errors $e_{v_i} := v_i - v_{d_i}$, and \hat{m}_i , $\hat{\alpha}_i$ denote the estimates of m_i and α_i , respectively, by agent i , evolving according to (12). We further denote $\hat{m} := [\hat{m}_1, \dots, \hat{m}_N]^\top$, $\hat{\alpha} := [\hat{\alpha}_1, \dots, \hat{\alpha}_N]^\top \in \mathbb{R}^N$. The following theorem considers the convergence of a leader to its destination.

Theorem 3 *Consider N robots operating in \mathcal{W} , subject to the uncertain 2nd-order dynamics (28), and a leader $i_{\mathcal{L}}$. Under Assumptions 1-4, the control protocol (30), (31), (12) guarantees collision avoidance between the agents*

and the agents and obstacles/workspace boundary as well as convergence of $x_{i_{\mathcal{L}}}$ to $x_{d_{i_{\mathcal{L}}}}$ from almost all initial conditions $(x(t_0), v(t_0), \hat{m}(t_0), \hat{\alpha}(t_0)) \in \mathcal{F} \times \mathbb{R}^{N(n+1)} \times \mathbb{R}_{\geq 0}^N$, given sufficiently small τ , $\tau_{i_{\mathcal{L}}}$, and that $k_{\phi_i} > \frac{\alpha_i}{2}$, $i \in \mathcal{N}$. Moreover, all closed loop signals remain bounded, $\forall t \geq t_0$.

Proof We prove first the avoidance of collisions by considering the function

$$V := \sum_{i \in \mathcal{N}} \left\{ k_{\phi_i} \phi_i + \frac{m_i}{2} \|e_{v_i}\|^2 + \frac{3}{4k_{\alpha_i}} \tilde{\alpha}_i^2 + \frac{1}{2k_{m_i}} \tilde{m}_i^2 \right\}.$$

Since $x(t_0) \in \mathcal{F}$, $V(t_0)$ is bounded. Differentiation of V yields, after using $\sum_{i \in \mathcal{N}} \sum_{j \in \mathcal{N} \setminus \{i\}} (x_i - x_j)^\top (v_i - v_j) = 2 \sum_{i \in \mathcal{N}} \sum_{j \in \mathcal{N} \setminus \{i\}} (x_i - x_j)^\top v_i$, (31), (12), and proceeding like in the proof of Theorem 1, yields

$$\begin{aligned} \dot{V} &= \sum_{i \in \mathcal{N}} \left\{ 2k_{\phi_i} k_{1_i} (x_i - x_{d_i}) - 2k_{\phi_i} k_{2_i} \left(\beta'_i(d_{i,o_0}) x - \sum_{k \in \mathcal{J}} \beta'_i(d_{i,o_k}) (x_i - c_k) \right. \right. \\ &\quad \left. \left. - 2 \sum_{j \in \mathcal{N} \setminus \{i\}} \beta'(d_{i,j}) (x_i - x_j) - \sum_{j \in \mathcal{N} \setminus \{i\}} k_{f_i} \beta'_i(d_{i,d_j}) (x_i - x_{d_j}) \right)^\top v_i + \right. \\ &\quad \left. e_{v_i}^\top (u_i - f_i(x_i, v_i) - m_i g - m_i \dot{v}_{d_i}) + \frac{1}{2k_{\alpha_i}} \tilde{\alpha}_i \dot{\tilde{\alpha}}_i + \frac{1}{2k_{m_i}} \tilde{m}_i \dot{\tilde{m}}_i \right\} \\ &\leq \sum_{i \in \mathcal{N}} \left\{ k_{\phi_i} \nabla_{x_i} \tilde{\phi}_i(x)^\top v_i + e_{v_i}^\top (u_i - m_i(g + \dot{v}_{d_i})) + \right. \\ &\quad \left. \alpha_i \|e_{v_i}\| \|v_i\| + \tilde{\alpha}_i \|e_{v_i}\|^2 - \tilde{m}_i e_{v_i}^\top (\dot{v}_{d_i} + g) \right\}, \end{aligned}$$

which, by using $v_i = e_{v_i} + v_{d_i}$ and substituting the control and adaptation laws (31), (12), becomes

$$\dot{V} \leq - \sum_{i \in \mathcal{N}} \left\{ \left(k_{\phi_i} - \frac{\alpha_i}{2} \right) \|\nabla_{x_i} \tilde{\phi}_i(x)\|^2 + k_{v_i} \|e_{v_i}\|^2 \right\} \leq 0,$$

and hence, $V(t) \leq V(t_0)$, which implies the boundedness of all closed-loop signals as well as that collisions between the agents and the agents and obstacles/workspace boundary are avoided $\forall t \geq t_0$. Moreover, following similar arguments as in the proof of Theorem 1, we conclude that $\lim_{t \rightarrow \infty} \|\nabla_{x_i} \tilde{\phi}_i(x(t))\| = \lim_{t \rightarrow \infty} \|e_{v_i}(t)\| = \lim_{t \rightarrow \infty} \|v_i(t)\| = \lim_{t \rightarrow \infty} \|\dot{v}_i(t)\| = 0$, $\forall i \in \mathcal{N}$. For the

followers $\mathcal{N}_{\mathcal{F}}$, depending on the choice of τ_i , $i \in \mathcal{N}_{\mathcal{F}}$, the critical point $\nabla_{x_i} \tilde{\phi}_i(x(t)) = 0$ might either correspond to their destination x_{d_i} or a local minimum. In any case, it holds that $x(t) \in \mathcal{F}$, $\forall t \geq t_0$, and hence, for all the followers $i \in \mathcal{N}_{\mathcal{F}}$,

$$\|x_i(t) - c_k\| > r_i + r_{o_k} + 2r_M + 2\bar{r}, \forall k \in \mathcal{J} \quad (32a)$$

$$\|x_i(t) - x_j(t)\| > r_i + r_j + 2r_M + 2\bar{r}, \forall j \in \mathcal{N}_{\mathcal{F}} \setminus \{i\} \quad (32b)$$

$$r_{\mathcal{W}} - \|x_i\| > r_i + 2r_M + 2\bar{r}, \quad (32c)$$

$$\|x_i(t) - x_{d_j}\| > r_i + r_j + 2r_M + 2\bar{r} + \varepsilon, \forall j \in \mathcal{N}_i \quad (32d)$$

$\forall t > t_0$. Hence, since $\lim_{t \rightarrow \infty} \|v_i(t)\| = \lim_{t \rightarrow \infty} \|\dot{v}_i(t)\| = 0$, $\forall i \in \mathcal{N}$, the multi-robot case reduces to the single-robot case of Section 4, where the followers resemble static obstacles. Note that the obstacle constraints (6) are always satisfied by the followers (see (32a)-(32c)); (32d) implies that the configuration that corresponds to the leader destination, i.e., $[x_1^\top, \dots, x_{i_{\mathcal{L}}-1}^\top, x_{d_{i_{\mathcal{L}}}}^\top, x_{i_{\mathcal{L}}+1}^\top, \dots, x_N^\top]^\top$, belongs always in its free space $\mathcal{F}_{i_{\mathcal{L}}}$. Hence, by choosing sufficiently small $\tau, \tau_{i_{\mathcal{L}}}$ in the interval $(0, \min(\bar{r}^2, \bar{r}_d))$, with \bar{r}_d as defined in (7), we guarantee the safe navigation of $x_{i_{\mathcal{L}}}$ to $x_{d_{i_{\mathcal{L}}}}$ from almost all initial conditions, as in Section 4.

When the current leader $i_{\mathcal{L}}$ reaches ε -close to its goal, at a time instant $t_{i_{\mathcal{L}}}$ ⁵, it broadcasts this information to the other agents, switches off its control and remains immobilized, considered hence as a static obstacle with center $c_{M+1} := x_{i_{\mathcal{L}}}(t_{i_{\mathcal{L}}})$ and radius r_{M+1} by the rest of the team. Note that $\|c_{M+1} - x_{d_{i_{\mathcal{L}}}}\| \leq \varepsilon$ and hence, in view of (29), $\|c_j - c_{M+1}\| > r_{o_j} + r_{i_{\mathcal{L}}} + 2r_M + 2\bar{r}$, $\forall j \in \mathcal{J}$, and $r_{\mathcal{W}} - \|c_{M+1}\| > r_{i_{\mathcal{L}}} + 2r_M + 2\bar{r}$, satisfying the obstacle spacing properties (6). The next agent $i'_{\mathcal{L}} \in \tilde{\mathcal{N}} := \mathcal{N} \setminus \{i_{\mathcal{L}}\}$ in priority is then assigned

⁵Note that the proven asymptotic stability of Theorem 3 guarantees that this will occur in finite time.

as a leader for navigation, and we redefine the sets

$$\begin{aligned}
\tilde{\mathcal{O}}_{i'_L, j} &:= \{q \in \bar{\mathcal{W}}_{i'_L} : \|q_i - c_j\| \leq r_{o_j} + r_i\}, \forall j \in \tilde{\mathcal{J}} \\
\tilde{\mathcal{C}}_{i'_L} &:= \{q \in \bar{\mathcal{W}}_{i'_L} : \|q_{i'_L} - q_j\| \leq r_{i'_L} + r_j, \forall j \in \tilde{\mathcal{N}} \setminus \{i'_L\}\}, \\
\tilde{\mathcal{O}}_{i, j} &:= \{q \in \bar{\mathcal{W}}_i : \|q_i - c_j\| \leq r_{o_j} + r_i + 2r_M + 2\bar{r}\}, \forall j \in \tilde{\mathcal{J}} \\
\tilde{\mathcal{C}}_i &:= \{q \in \bar{\mathcal{W}}_i : \|q_i - q_{i'_L}\| \leq r_i + r_{i'_L}, \\
&\quad \|q_i - q_j\| \leq r_i + r_j + 2r_M + 2\bar{r}, \forall j \in \tilde{\mathcal{N}} \setminus \{i'_L, i\}, \\
&\quad \|q_i - x_{d_j}\| \leq r_i + r_j + 2r_M + 2\bar{r} + \varepsilon, \forall j \in \tilde{\mathcal{N}}_i\},
\end{aligned}$$

$\forall i \in \tilde{\mathcal{N}} \setminus \{i'_L\}$, where $\tilde{\mathcal{N}}_i := \mathcal{N}_i \setminus \{i_L\}$, and $\tilde{\mathcal{J}} := \mathcal{J} \cup \{M+1\}$, to account for the new obstacle $M+1$. The new free space is $\tilde{\mathcal{F}}_i := \bar{\mathcal{W}}_i \setminus \{(\bigcup_{j \in \tilde{\mathcal{J}}} \tilde{\mathcal{O}}_{i, j}) \cup \tilde{\mathcal{C}}_i\}$, $\forall i \in \tilde{\mathcal{N}}$ and, in view of (32), one can conclude that $x_{i'_L}(t_{i_L}) \in \tilde{\mathcal{F}}_{i'_L}$, $x_i(t_{i_L}) \in \tilde{\mathcal{F}}_i \forall i \in \tilde{\mathcal{N}} \setminus \{i'_L\}$. Therefore, the application of Theorem 3 with t_{i_L} as t_0 and agent i'_L as leader guarantees its navigation ε -close to $x_{d_{i'_L}}$. Applying iteratively the aforementioned reasoning, we guarantee the successful navigation of all the agents to their destinations.

7 Simulation Results

This section verifies the theoretical findings of Sections 4-6 via computer simulations. We consider first a 2D workspace on the horizontal plane with $r_W = 11$, populated with $M = 60$ randomly placed obstacles, whose radius, enlarged by the robot radius, is randomly chosen in $\bar{r}_{o_j} \in [0.25, 0.75]$, $\forall j \in \mathcal{J}$. The mass, is chosen as $m = 1$, and $f(x, v) = \frac{\alpha}{16} \sin(0.5(x_1 + x_2))F(v)v$, with $F(v) = \text{diag}\{\exp(-\text{sgn}(v_i)v_i) + 1\}_{i \in \{1, 2\}}$, and $\alpha = 10$, where we denote $(x_1, x_2) = x$, $(v_1, v_2) = v$. Note that $f(\cdot)$ is highly nonlinear, motivated by the friction model of [44]. We choose the goal position as $x_d = (5, 5)$, which the robot aims to converge to from 3 different initial positions, namely $x(0) = -(5, 5)$, $(-7, 3.5)$, and $(3.5, -7)$. The parameter \bar{r} is chosen as $\bar{r} = 0.5$. We choose a variation of (8) for β with $\tau = \bar{r}^2$. The control gains are chosen as $k_1 = 0.04$, $k_2 = 5$, $k_v = 20$, $k_\phi = 1$, and $k_m = k_\alpha = 0.01$. The results for $t \in [0, 100]$ seconds are depicted in Figs. 1, 2; 1 (left) shows that the robot navigates to its destination without any collisions, and 2 depicts the input and adaptation signals $u(t)$, $\hat{\alpha}(t)$, $\hat{m}(t)$ for the trajectory starting from $(-5, 5)$. In addition, note that the fact that $\alpha > 2$ does not affect the performance

of the proposed control protocol and hence we can verify that the condition $k_\phi > \frac{\alpha}{2}$ is only sufficient and not necessary. Moreover, in order to verify the results of Section 4, we add a bounded time-varying disturbance vector $d(x, v, t) = d(t) := 2 [\sin(0.5t + \frac{\pi}{3}), \cos(0.4t - \frac{\pi}{4})]^\top \in \mathbb{R}^2$ and we choose the extra control gains as $\sigma_m = \sigma_\alpha = 0.1$. The results are depicted in Fig. 1 (right), which shows the safe navigation of the agent to a set close to x_d , and Fig. 2, which shows the input and adaptation signals for the trajectory starting from $(-5, 5)$.

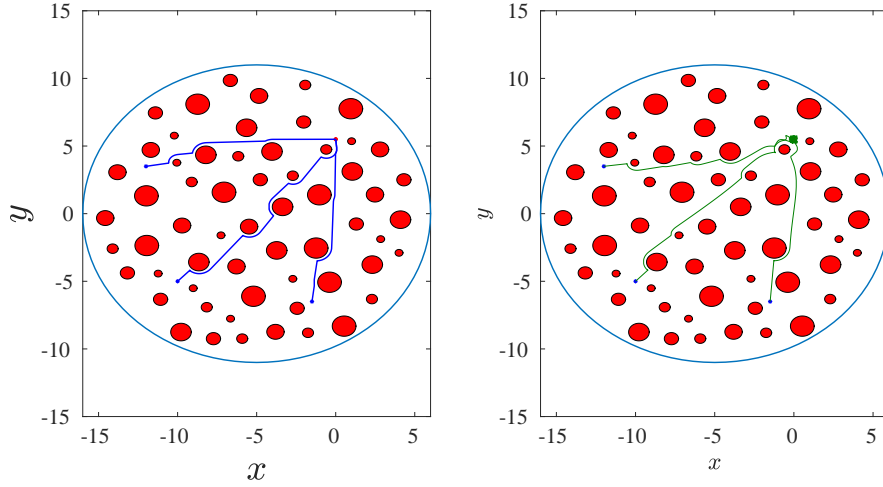


Figure 1: The resulting trajectories $x(t)$, $t \in [0, 100]$ seconds, from the initial points $(-5, 5)$, $(-7, 3.5)$, and $(3.5, -7)$ to the destination $(5, 5)$. Left: without any disturbances. Right: with bounded disturbance $d(x, v, t)$.

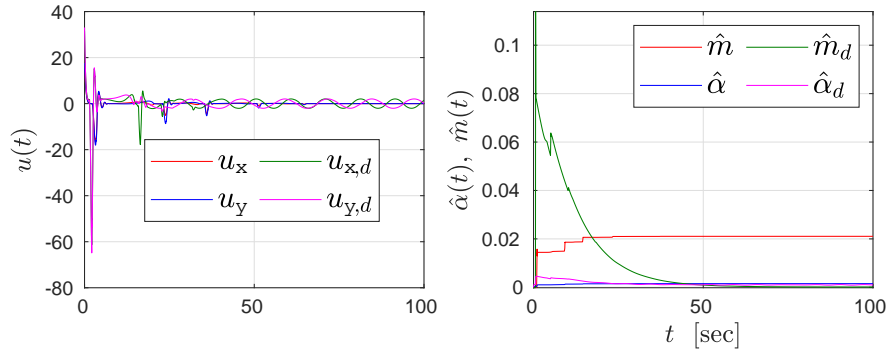


Figure 2: The input $u(t) = (u_1(t), u_2(t))$ (left), and adaptation signals $\hat{\alpha}(t)$, $\hat{m}(t)$ (right) for the 2D trajectory from $(-5, 5)$ to $(5, 5)$ of Fig. 1. The subscript d corresponds to the model where a bounded disturbance vector $d(x, v, t)$ was included.

Next, we consider a 3D workspace with $r_{\mathcal{W}} = 11$, populated with $M = 200$ randomly placed obstacles, whose radius, enlarged by the robot radius, is randomly chosen in $\bar{r}_{o_j} \in [0.25, 0.75]$, $\forall j \in \mathcal{J}$; $f(x, v)$ and m as well as the β functions and control gains are chosen as in the 2D scenario. We choose the goal position as $x_d = (4, 4, 4)$, which the robot aims to converge to from 3 different initial positions, namely $x(0) = -(4, 4, 4)$, $(-4, 4, -4)$, and $(-4, -4, 4)$. The parameter \bar{r} is chosen as $\bar{r} = 0.75$. The robot navigation as well as the input and adaptation signals $u(t)$, $\hat{\alpha}(t)$, $\hat{m}(t)$ (for the trajectory starting from $-(4, 4, 4)$) are depicted in Figs. 3, and 4 for $t \in [0, 100]$ seconds. Note that the robot navigates to its destination without any collisions and that \hat{m} converges to m , as predicted by the theoretical results.

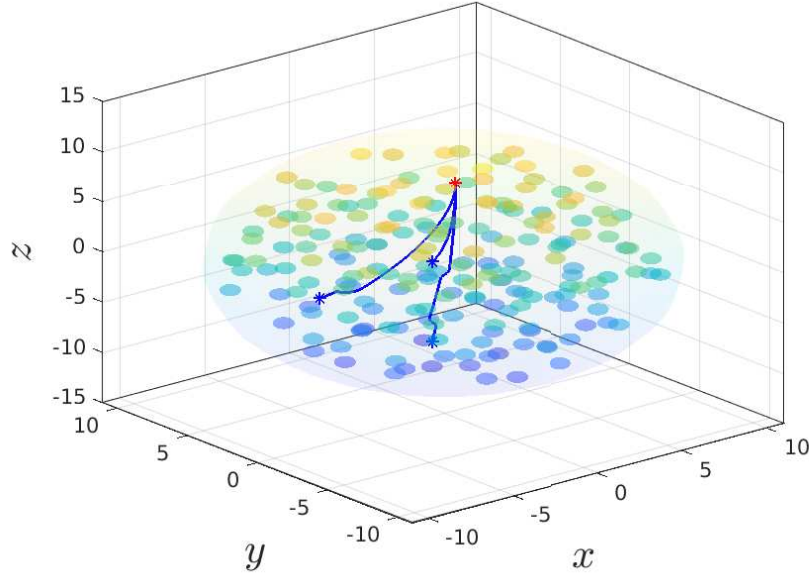


Figure 3: The resulting trajectories $x(t)$, $t \in [0, 100]$ seconds, from the initial points $-(4, 4, 4)$, $(-4, -4, 4)$, and $(-4, 4, -4)$ to the destination $(4, 4, 4)$.

Next, we illustrate the performance of the control protocol of Section 5 in a 2D star-world. We consider a workspace with $r_{\mathcal{W}} = 8$, which contains 2 star-shaped obstacles, centered at $(-3, -3)$ and $(0, 1)$, respectively. The mass m and function $f(x, v)$ are given as before, with $\alpha = 1$. In order to transform the workspace to a sphere world, we employ the transformation proposed in [4]. In the transformed sphere world, we choose $\bar{r} = 4$ and $\bar{r}_{o_j} = 0.5$, whereas the function β is chosen as in the sphere-world case. The initial and goal

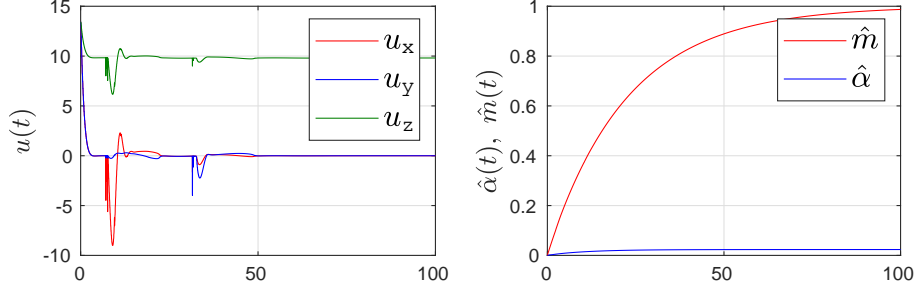


Figure 4: The input $u(t) = (u_1(t), u_2(t))$ (left), and adaptation signals $\hat{\alpha}(t)$, $\hat{m}(t)$ (right) for the 3D trajectory from $(-4, 4, 4)$ to $(4, 4, 4)$ of Fig. 3.

position are selected as $x(0) = (-5, -5)$ and $x_d = (3, 4)$, respectively, and the control gains as $k_1 = 0.04$, $k_2 = .2$, $k_v = 20$, $k_\phi = 1$, and $k_m = k_\alpha = 0.01$. The robot trajectory is depicted in Fig. 5, for $t \in [0, 500]$ seconds, both in the original star and in the transformed sphere world.

Finally, we use the control scheme of Section 6 in a multi-agent scenario. We consider 20 agents in a 2D workspace of $r_W = 120$, populated with 70 obstacles. The agents and obstacles are randomly initialized to satisfy the conditions of the free space of Section 6, as shown in Fig. 6. The radius of the agents and the obstacles is chosen as $r_i = r_{o_j} = 2$, $\forall i \in \mathcal{N}, j \in \mathcal{J}$, and the sensing radius of the agents is taken as $\varsigma_i = 20$, $\forall i \in \mathcal{N}$. The functions β , β_i are chosen as before, and we also choose $\bar{r} = 4$, $\varepsilon = 0.1$. The results are depicted in Fig. 7 for 870 seconds, which shows the convergence of the distance errors $\|x_i(t) - x_{d-i}\|$ to zero, $\forall i \in \mathcal{N}$ as well as the minimum of the distances $\|x_i(t) - x_j(t)\| - 2r$, $\forall i, j \in \mathcal{N}$, $i \neq j$, and $\|x_i(t) - c_j\| - 2r$, $\forall i \in \mathcal{N}, j \in \mathcal{J}$, defined as $\beta_{\min}(t) := \min\{\min_{i,j \in \mathcal{N}, i \neq j} \{\|x_i(t) - x_j(t)\| - 2r\}, \min_{(i,j) \in \mathcal{N} \times \mathcal{J}} \{\|x_i(t) - c_j\| - 2r\}\}$, which stays strictly positive, $\forall t \in [0, 870]$, implying that collisions are avoided. A video illustrating the multi-agent navigation can be found in <https://vimeo.com/393443782>.

8 Conclusion and Future Work

This paper considers the robot navigation in an obstacle-cluttered environment subject to uncertain 2nd-order dynamics. A novel navigation function is proposed and combined with adaptation laws that compensate for the uncertain dynamics. The results are extended to star worlds as well as multi-agent cases. Future directions will aim at relaxing the assumptions for the latter.

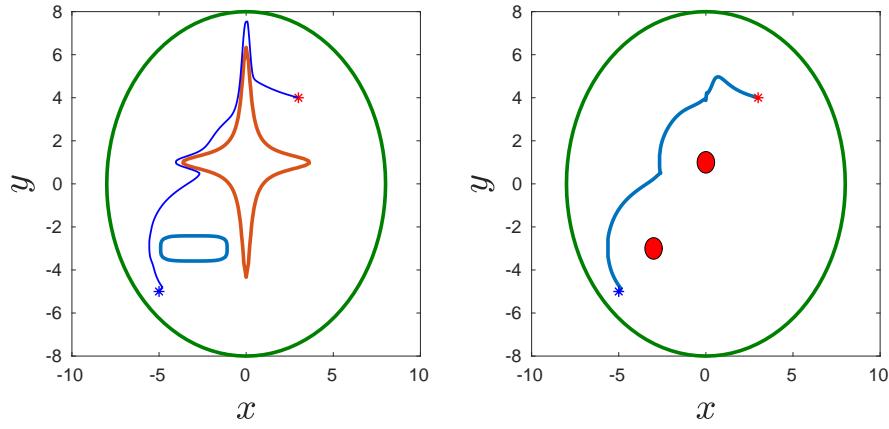


Figure 5: The resulting trajectory $x(t)$, $t \in [0, 500]$ seconds, from the initial points $(-5, -5)$ to the destination $(3, 4)$, in the 2D star world workspace (left) and the transformed sphere world (right).

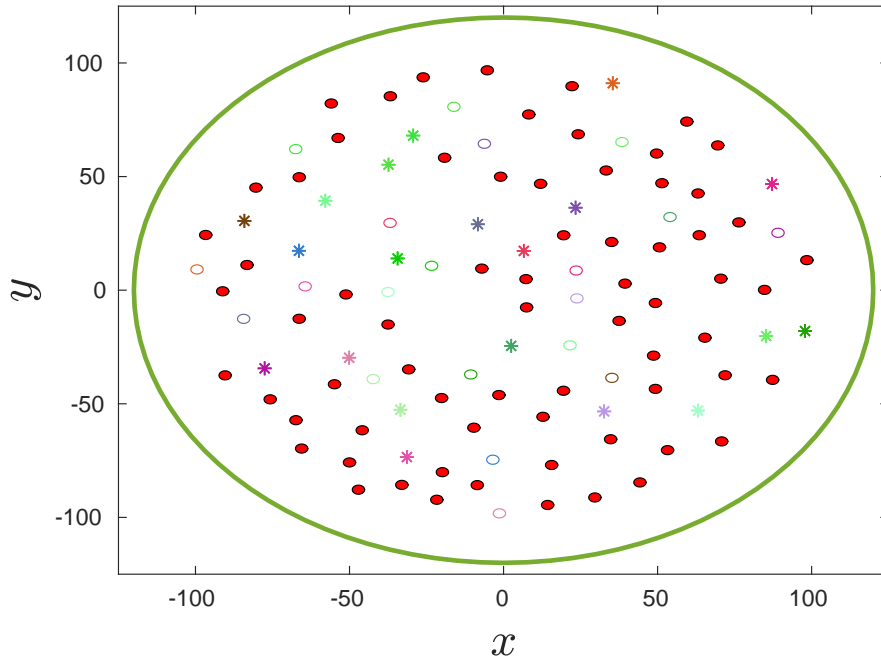


Figure 6: The initial configurations of the multi-agent scenario. The obstacles are depicted as filled red disks whereas the agents as circles. The destinations are shown with asterisk.

References

- [1] Vladimir J Lumelsky. *Sensing, intelligence, motion: how robots and humans move in an unstructured world*. John Wiley & Sons, 2005.

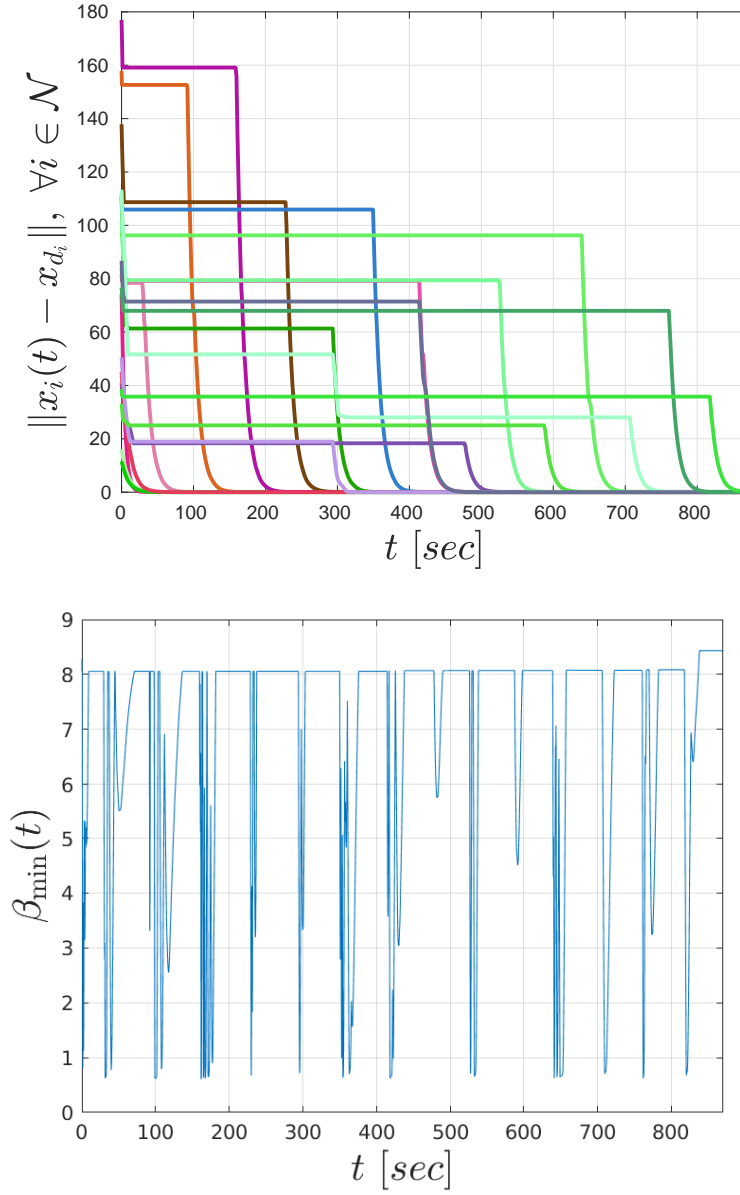


Figure 7: The resulting signals $\|x_i(t) - x_{d_i}\|$, $\forall i \in \mathcal{N}$ (left) and the signal $\beta_{\min}(t)$ (right).

- [2] Steven M LaValle. *Planning algorithms*. Cambridge university press, 2006.
- [3] Daniel E Koditschek and Elon Rimon. Robot navigation functions on manifolds with boundary. *Advances in applied mathematics*, 11(4):412–

442, 1990.

- [4] Elon Rimon and Daniel E Koditschek. Exact robot navigation using artificial potential functions. *Transactions on Robotics and Automation*, 8(5):501–518, 1992.
- [5] Ioannis Filippidis and Kostas J Kyriakopoulos. Adjustable navigation functions for unknown sphere worlds. *2011 50th IEEE Conference on Decision and Control and European Control Conference*, pages 4276–4281, 2011.
- [6] Dimos V Dimarogonas, Savvas G Loizou, Kostas J Kyriakopoulos, and Michael M Zavlanos. A feedback stabilization and collision avoidance scheme for multiple independent non-point agents. *Automatica*, 42(2):229–243, 2006.
- [7] Christos K Verginis, Ziwei Xu, and Dimos V Dimarogonas. Decentralized motion planning with collision avoidance for a team of uavs under high level goals. *ICRA*, pages 781–787, 2017.
- [8] Christos K Verginis and Dimos V Dimarogonas. Robust decentralized abstractions for multiple mobile manipulators. *CDC*, pages 2222–2227, 2017.
- [9] Giannis Roussos and Kostas J Kyriakopoulos. Decentralized and prioritized navigation and collision avoidance for multiple mobile robots. *Distributed Autonomous Robotic Systems*, pages 189–202, 2013.
- [10] Santiago Paternain, Daniel E Koditschek, and Alejandro Ribeiro. Navigation functions for convex potentials in a space with convex obstacles. *IEEE Transactions on Automatic Control*, 63(9):2944–2959, 2017.
- [11] Herbert G Tanner and Amit Kumar. Towards decentralization of multi-robot navigation functions. *ICRA*, 4:4132, 2005.
- [12] Dimitra Panagou. A distributed feedback motion planning protocol for multiple unicycle agents of different classes. *IEEE Transactions on Automatic Control*, 62(3):1178–1193, 2017.
- [13] Savvas G Loizou. The navigation transformation. *IEEE Transactions on Robotics*, 33(6):1516–1523, 2017.

- [14] Panagiotis Vlantis, Constantinos Vrohidis, Charalampos P Bechlioulis, and Kostas J Kyriakopoulos. Robot navigation in complex workspaces using harmonic maps. *2018 IEEE International Conference on Robotics and Automation (ICRA)*, pages 1726–1731, 2018.
- [15] Paweł Szulczyński, Dariusz Pazderski, and Krzysztof Kozłowski. Real-time obstacle avoidance using harmonic potential functions. *Journal of Automation Mobile Robotics and Intelligent Systems*, 5:59–66, 2011.
- [16] Savvas G Loizou. The multi-agent navigation transformation: Tuning-free multi-robot navigation. *Robotics: Science and Systems*, 6:1516–1523, 2014.
- [17] Constantinos Vrohidis, Panagiotis Vlantis, Charalampos P Bechlioulis, and Kostas J Kyriakopoulos. Prescribed time scale robot navigation. *IEEE Robotics and Automation Letters*, 3(2):1191–1198, 2018.
- [18] Li Wang, Aaron D Ames, and Magnus Egerstedt. Safety barrier certificates for collisions-free multirobot systems. *IEEE Transactions on Robotics*, 33(3):661–674, 2017.
- [19] Alexandros Filotheou, Alexandros Nikou, and Dimos V Dimarogonas. Decentralized control of uncertain multi-agent systems with connectivity maintenance and collision avoidance. *European Control Conference*, 2018.
- [20] José M Mendes Filho, Eric Lucet, and David Filliat. Real-time distributed receding horizon motion planning and control for mobile multi-robot dynamic systems. *ICRA*, pages 657–663, 2017.
- [21] Christos K Verginis, Alexandros Nikou, and Dimos V Dimarogonas. Communication-based decentralized cooperative object transportation using nonlinear model predictive control. *2018 European Control Conference (ECC)*, pages 733–738, 2018.
- [22] Daniel Morgan, Giri P Subramanian, Soon-Jo Chung, and Fred Y Hadaegh. Swarm assignment and trajectory optimization using variable-swarm, distributed auction assignment and sequential convex programming. *IJRR*, 35(10):1261–1285, 2016.

- [23] Jur Van Den Berg, Jamie Snape, Stephen J Guy, and Dinesh Manocha. Reciprocal collision avoidance with acceleration-velocity obstacles. *ICRA*, 2011.
- [24] Javier Alonso-Mora, Andreas Breitenmoser, Martin Rufli, Roland Siegwart, and Paul Beardsley. Image and animation display with multiple mobile robots. *The International Journal of Robotics Research*, 31(6):753–773, 2012.
- [25] Sotiris Stavridis, Dimitrios Papageorgiou, and Zoe Doulgeri. Dynamical system based robotic motion generation with obstacle avoidance. *IEEE Robotics and Automation Letters*, 2(2):712–718, 2017.
- [26] V Grushkovskaya and A Zuyev. Obstacle avoidance problem for second degree nonholonomic systems. *2018 IEEE Conference on Decision and Control*, 2018.
- [27] Jan Maximilian Montenbruck, Mathias Bürger, and Frank Allgöwer. Navigation and obstacle avoidance via backstepping for mechanical systems with drift in the closed loop. *2015 American Control Conference (ACC)*, pages 625–630, 2015.
- [28] Omur Arslan and Daniel E Koditschek. Exact robot navigation using power diagrams. *ICRA*, pages 1–8, 2016.
- [29] Omur Arslan, Dan P Guralnik, and Daniel E Koditschek. Coordinated robot navigation via hierarchical clustering. *IEEE Transactions on Robotics*, 32(2):352–371, 2016.
- [30] Soulaïmane Berkane, Andrea Bisoffi, and Dimos V Dimarogonas. A hybrid controller for obstacle avoidance in an n-dimensional euclidean space. *2019 European Control Conference (ECC)*, 2019.
- [31] Lukas Huber, Aude Billard, and Jean-Jacques Slotine. Avoidance of convex and concave obstacles with convergence ensured through contraction. *2019 IEEE International Conference on Robotics and Automation*, 2019.
- [32] Daniel E Koditschek. The control of natural motion in mechanical systems. *Journal of dynamic systems, measurement, and control*, 113(4):547–551, 1991.

- [33] Savvas G Loizou. Closed form navigation functions based on harmonic potentials. *Conference on Decision and Control and European Control Conference*, pages 6361–6366, 2011.
- [34] Omur Arslan and Daniel E Koditschek. Smooth extensions of feedback motion planners via reference governors. *ICRA*, pages 4414–4421, 2017.
- [35] Chien Chern Cheah, Saing Paul Hou, and Jean Jacques E Slotine. Region-based shape control for a swarm of robots. *Automatica*, 45(10):2406–2411, 2009.
- [36] Christos K. Verginis and Dimos V. Dimarogonas. Closed-form barrier functions for multi-agent ellipsoidal systems with uncertain lagrangian dynamics. *IEEE Control Systems Letters (L-CSS)*, 2019.
- [37] C Makkar, WE Dixon, WG Sawyer, and G Hu. A new continuously differentiable friction model for control systems design. *IEEE/ASME International Conference on Advanced Intelligent Mechatronics.*, pages 600–605, 2005.
- [38] Grigoris Lionis, Xanthi Papageorgiou, and Kostas J Kyriakopoulos. Locally computable navigation functions for sphere worlds. *IEEE International Conference on Robotics and Automation*, pages 1998–2003, 2007.
- [39] Eugene Lavretsky and Kevin A Wise. Robust adaptive control. *Robust and adaptive control*, pages 317–353, 2013.
- [40] Yuri A Kuznetsov. *Elements of applied bifurcation theory*, volume 112. Springer Science & Business Media, 2013.
- [41] Hassan K Khalil. Nonlinear systems. *Prentice-Hall, New Jersey*, 2(5):5–1, 1996.
- [42] Elon Rimon and Daniel E Koditschek. The construction of analytic diffeomorphisms for exact robot navigation on star worlds. *Transactions of the American Mathematical Society*, 327(1):71–116, 1991.
- [43] Meng Guo, Jana Tumova, and Dimos V Dimarogonas. Communication-free multi-agent control under local temporal tasks and relative-distance constraints. *IEEE Transactions on Automatic Control*, 61(12):3948–3962, 2016.

- [44] C Canudas De Wit, Hans Olsson, Karl Johan Astrom, and Pablo Lischinsky. A new model for control of systems with friction. *IEEE Transactions on automatic control*, 40(3):419–425, 1995.